Genetic analysis of praziquantel response in schistosome parasites implicates a Transient Receptor Potential channel

Winka Le Clec'h[1*§], Frédéric D. Chevalier[1§], Ana Carolina A. Mattos[2], Amanda Strickland[1], Robbie Diaz[1], Marina McDew-White[1], Claudia M. Rohr[3], Safari Kinung'hi [4], Fiona Allan[5,6], Bonnie L Webster [5,6], Joanne P Webster [5,7], Aidan M Emery [5,6], David Rollinson [5,6], Amadou Garba Djirmay [8,9], Khalid M Al Mashikhi [10], Salem Al Yafae [10], Mohamed A Idris [11], Hélène Moné [12], Gabriel Mouahid [12], Philip LoVerde[2], Jonathan S. Marchant[3], Timothy J.C. Anderson[1*]

[1] Texas Biomedical Research Institute; San Antonio, TX

[2] University of Texas Health Science Center at San Antonio; San Antonio, TX 78229

[3]Department of Cell Biology, Neurobiology and Anatomy, Medical College of Wisconsin; Milwaukee WI 53226, USA.

[4] National Institute for Medical Research, Mwanza, United Republic of Tanzania

[5] London Centre for Neglected Tropical Disease Research (LCNDTR), Imperial College, London, United Kingdom

[6] Wolfson Wellcome Biomedical Laboratories, Natural History Museum, London, United Kingdom

[7] Centre for Emerging, Endemic and Exotic Diseases (CEEED), Royal Veterinary College, University of London, United Kingdom

[8] Réseau International Schistosomiases Environnemental Aménagement et Lutte (RISEAL), Niamey, Niger

[9] World Health Organization, Geneva, Switzerland

[10] Directorate General of Health Services, Dhofar Governorate, Salalah, Sultanate of Oman

[11] Sultan Qaboos University, Muscat, Sultanate of Oman

[12] Host-Pathogen-Environment Interactions laboratory, University of Perpignan, Perpignan, France

[§] These authors contributed equally to this work.

27 *Correspondence to: winkal@txbiomed.org (WL), tanderso@txbiomed.org (TA)

Abstract:

Mass treatment with praziquantel (PZQ) monotherapy is the mainstay for schistosomiasis treatment. This drug shows imperfect cure rates in the field and parasites showing reduced PZQ response can be selected in the laboratory, but the extent of resistance in *Schistosoma mansoni* populations is unknown. We examined the genetic basis of variation in PZQ response in a *S. mansoni* population (SmLE-PZQ-R) selected with PZQ in the laboratory: 35% of these worms survive high dose (73 µg/mL) PZQ treatment. We used genome wide association to map loci underlying PZQ response. The major chr. 3 peak contains a transient receptor potential (*Sm.TRPM*$_{PZQ}$) channel (Smp_246790), activated by nanomolar concentrations of PZQ. PZQ response shows recessive inheritance and marker-assisted selection of parasites at a single *Sm.TRPM*$_{PZQ}$ SNP enriched populations of PZQ-resistant (PZQ-ER) and sensitive (PZQ-ES) parasites showing >377 fold difference in PZQ response. The PZQ-ER parasites survived treatment in rodents better than PZQ-ES. Resistant parasites show 2.25-fold lower expression of *Sm.TRPM*$_{PZQ}$ than sensitive parasites. Specific chemical blockers of *Sm.TRPM*$_{PZQ}$ enhanced PZQ resistance, while *Sm.TRPM*$_{PZQ}$ activators increased sensitivity. A single SNP in *Sm.TRPM*$_{PZQ}$ differentiated PZQ-ER and PZQ-ES lines, but mutagenesis showed this was not involved in PZQ-response, suggesting linked regulatory changes. We surveyed *Sm.TRPM*$_{PZQ}$ sequence variation in 259 parasites from the New and Old World revealing one nonsense mutation that results in a truncated protein with no PZQ-binding site. Our results demonstrate that *Sm.TRPM*$_{PZQ}$ underlies variation in PZQ response in *S. mansoni* and provides an approach for monitoring emerging PZQ-resistance alleles in schistosome elimination programs.

One Sentence Summary: A transient receptor potential channel determines variation in praziquantel-response in *Schistosoma mansoni*.

INTRODUCTION

Praziquantel (PZQ) is the drug of choice for treating schistosomiasis, a snail vectored parasitic disease, caused by flatworms in the genus *Schistosoma*. Schistosomiasis is widespread: three main parasite species infect over 140 million people in Africa, the Middle-East, South America and Asia *(1, 2)*, resulting in widespread morbidity – a global burden of 1.9 million disability adjusted life years *(3)* – and mortality estimates ranging from 20,000 to 280,000 people annually *(4, 5)*. Pathology results from eggs that lodge in the liver and intestine (*S. mansoni* and *S. japonicum*) or in the urogenital system (*S. haematobium*) stimulating granuloma formation. This results in a spectrum of pathology including portal hypertension, hepatosplenic disease, bladder cancer, genital schistosomiasis and infertility. *S. mansoni* infection alone results in a conservative estimate of 8.5 million cases of hepatosplenomegaly in sub-Saharan Africa *(6)*. Mass drug administration programs currently distribute an estimated 250 million doses of PZQ per year aimed in the short term at reducing schistosome associated morbidity and mortality, and in the longer term at eliminating schistosomiasis transmission *(7, 8)*. PZQ is also widely used for treatment of other flatworm parasites of both humans and livestock including tapeworms.

PZQ treatment of adult worms results in rapid Ca^{2+} influx into cells, muscle contraction and tegument damage *(9–12)*. Both the mechanism of action and the mechanism of resistance to PZQ have been the focus for much speculation and research *(13, 14)*. Several proteins like voltage-gated calcium channels *(15–17)* or ABC transporters *(18, 19)* have been suspected to play a role in PZQ resistance. However, this topic has been stimulated by the recent finding that a transient receptor channel (*Sm.TRPM*$_{PZQ}$) is activated by nanomolar quantities of PZQ *(20, 21)*.

Mass drug treatment with PZQ has enormous health benefits and has been extremely effective in reducing parasite burdens and transmission *(8)*, but imposes strong selection for resistance on treated schistosome populations. Emergence of PZQ resistance is a major concern, because it could derail current progress towards the WHO goal of eliminating schistosomiasis as a public health problem by 2025 *(8)*.

Several lines of evidence from both the field and the laboratory suggest that PZQ response varies in schistosome populations *(22–27)*. PZQ resistance is readily selected in the laboratory through treatment of infected rodents or infected intermediate snail hosts *(28)*. This typically results in a modest change (3-5 fold) in PZQ response in parasite populations *(28)*, although the PZQ resistance status of individual worms comprising these populations is unknown. PZQ treatment typically results in ~30% of patients who remain egg positive following treatment *(29)*. PZQ kills adult worms, but not immature parasites *(30, 31)*, so both newly emerging adult parasites and drug resistance may contribute to treatment failure. There have been several reports of patients who remained egg positive across multiple PZQ treatment cycles *(32, 33)*: schistosome infections established in mice from infective larvae from these patients showed elevated resistance to PZQ *(24, 34)*. In Kenya and Uganda, infected communities where prevalence and disease burden are not reduced by repeated treatment have been identified. The causes of these "hotspots" *(35, 36)* is currently unknown, but PZQ-resistant schistosomes are one explanation. In a large longitudinal study of individual school age children, egg reduction ratios (ERR) were high in naïve populations treated with PZQ, but showed a significant decline after multiple rounds of treatment *(37)*, consistent with selection of tolerance or resistance to PZQ. Identification of molecular markers for direct screening of levels of PZQ resistance alleles would be extremely valuable for parasite control programs, because changes in schistosome ERR have both genetic and non-genetic explanations and are laborious to measure.

The availability of good genome sequence and near complete genome assembly *(38)* for *S. mansoni* make unbiased genome wide approaches feasible for schistosome research *(39)*. Our central goal is to determine the genetic basis of variation in PZQ response, using genome wide association approaches. We exploit the PZQ-resistant parasites generated by laboratory selection *(26)* to determine the genetic basis of PZQ, identifying a transient receptor channel as the cause of variation in PZQ response. The Transient Receptor Potential Melastatin (TRPM) ion channel identified is activated by PZQ *(20, 21)* and has been designated *Sm.TRPM*$_{PZQ}$. Together, our genetic analysis and the independent

101 pharmacological analysis by Park *et al. (21)* identify the target channel for PZQ and provide a framework

102 for monitoring PZQ resistance evolution in schistosomiasis control programs.

RESULTS

PZQ resistant parasites are present in laboratory schistosome populations

Male and female schistosome parasites pair in the blood vessels and reproduction is obligately sexual, so schistosomes are maintained in the laboratory as outbred populations. Hence, individual parasites within laboratory populations may vary in PZQ response. We measured PZQ response in the SmLE-PZQ-R population, which was previously generated by PZQ treatment of infected snails *(26)*. This revealed a 14-fold difference in IC_{50} between the SmLE progenitor parasite population (IC_{50}=0.86 ± 0.14 µg/mL) and SmLE-PZQ-R (IC_{50}=12.75 ± 4.49 µg/mL, χ^2 test, p = 0.001) derived by PZQ selection (Fig. 1). This is higher than the 3-5 fold differences observed between PZQ-selected and unselected parasite populations in previous studies *(40)*. Interestingly, the dose response curve for the SmLE-PZQ-R population plateaus at 65% mortality: the remaining 35% of parasites recovered even at high dose of PZQ (72.9 µg/mL). These results suggest that the SmLE-PZQ-R parasite population is a mixed population that contains both PZQ-sensitive and PZQ-resistant individual worms (Fig. 1).

Association mapping of PZQ resistant genes identifies a TRPM channel

We conducted a genome wide association study (GWAS) to determine the genetic basis of PZQ resistance (PZQ-R). GWAS has been widely used for mapping drug resistance in parasitic protozoa *(41)* and the model nematode *Caenorhabditis elegans (42)*, but has not previously been applied to parasitic helminths, because of the difficulty of accurately measuring drug response in individual parasites. When worms are treated with PZQ, there is a massive influx of Ca^{2+} into cells and parasites contract *(17, 43)*, but some worms recover and resume respiration and movement 24-48h after drug removal. We assayed parasite recovery following high dose PZQ treatment (24 µg/mL) of individual male worms maintained in 96-well plates by measuring L-lactate production *(44)*, a surrogate measure of respiration, 48h after PZQ

126 treatment removal (Fig. S1). These assays allow efficient measurement of recovery in individual PZQ-
127 treated worms.

128 We conducted replicate experiments (A: n = 590; B: n = 691) to measure PZQ response in
129 individual parasites maintained in 96-well plates. The distributions of L-lactate production in the two
130 experiments were broad (A: 0-126.56 nmol/h, mean = 42.95 nmol/h; B: 0-118.61 nmol/h, mean = 37.79
131 nmol/h): we identified worms from the top and bottom quintile for L-lactate production (Fig. 2A) which
132 were then bulk sequenced to high read depth (average read depth - A: 39.97; B: 36.83). Two genome
133 regions (chr. 2 and chr. 3) showed strong differentiation in allele frequencies between parasite populations
134 showing high and low L-lactate production phenotypes (Fig. 2B). The highest peak ($p = 1.41 \times 10^{-22}$) on
135 chr. 3 spanned 4 Mb (22,805-4,014,031 bp) and contained 91 genes, of which 85 are expressed in adult
136 worms (Fig. 2C). This genome region contains several potential candidate loci including three partial
137 ABC transporters and a voltage-gated calcium channel subunit (Table S1). One gene close to the highest
138 association peak is of particular interest: Smp_246790 is a transient receptor potential channel in the M
139 family (TRPM). This same channel was recently shown to be activated by PZQ following exposure to
140 nanomole quantities of drug resulting in massive Ca^{2+} influx into HEK293 cells transiently expressing
141 this protein *(20, 21)*. This gene, designated *Sm.TRPM*$_{PZQ}$, is therefore a strong candidate to explain
142 variation in PZQ response within parasite populations. Two other features of the data are of interest. First,
143 the SNP (position 1029621 T>C) marking the highest association peak (at 1,030 Mb) is found in a
144 transcription factor (Smp_345310, SOX13 homology) from a family known to regulate splicing variants
145 *(45)*. Second, there is a ~150 kb deletion (1220683-1220861 bp) 6.5 kb from *Sm.TRPM*$_{PZQ}$ and another
146 150 kb deletion (1,200,000-1,350,000 bp) 170 kb from the transcription factor. This was enriched in high
147 L-lactate groups in both replicates and is in linkage disequilibrium with the enriched SNP in
148 *Sm.TRPM*$_{PZQ}$.

The chr. 2 peak ($p < 1.0 \times 10^{-15}$) spans 1.166 Mb (291,191-1,457,462 bp) and contains 24 genes (21 expressed in adult worms) (Table S1). This genome region does not contain obvious candidate genes that might explain variation in PZQ response.

PZQ resistance shows recessive inheritance

To confirm these associations and determine whether the loci underlying PZQ response are inherited in a dominant, co-dominant or recessive manner, we compared genotype and PZQ-response phenotype in individual worms. We compared the L-lactate production phenotypes of individual worms maintained in 96-well plates 48 hours after exposure to 24 µg/mL PZQ with their genotypes at SNPs at the peaks of the chr. 2 and chr. 3 QTLs. We also examined copy number of one of the 150 kb deletion observed on chr. 3 using qPCR. We observed significant differences in L-lactate production among genotypes (Fig. 3). Both the SNP assayed in *Sm.TRPM*$_{PZQ}$ and the copy number variant revealed that the causative gene in the chr. 3 QTL showed recessive inheritance (Fig 3B-C). Homozygous parasites carrying two copies of the *Sm.TRPM*$_{PZQ}$-741987C allele (or two copies of the deletion) recovered from PZQ treatment, while the heterozygotes and other homozygotes failed to recover from treatment (Fig. 3B-C). For the chr. 2 QTL, we did not see a significant association between parasite genotype and PZQ-R phenotype nor with L-lactate production before PZQ treatment (Fig. 3A): this locus was not investigated further.

Marker-assisted purification of resistant and sensitive parasites

As the chr. 3 QTL containing *Sm.TRPM*$_{PZQ}$ exhibits the strongest association with PZQ response and shows recessive inheritance, we were able to use single generation marker assisted selection approach to enrich parasites for alleles conferring PZQ resistance (PZQ-R) and PZQ sensitivity (PZQ-S) from the mixed genotype SmLE-PZQ-R parasite population (Fig. 4A). We genotyped clonal cercariae larvae

emerging from snails previously exposed to single miracidia to identify parasites homozygous for the recessive PZQ-R allele from those homozygous for the PZQ-S allele. Parasites isolated from multiple snails falling into these two alternative genotypes were then used to infect hamsters. The enriched PZQ-resistant and sensitive parasites were designated SmLE-PZQ-ER and SmLE-PZQ-ES. Sequencing of adult parasites recovered from these two populations revealed that they were fixed for alternative alleles at the *Sm.TRPM$_{PZQ}$*-741987C SNP genotyped, but showed similar allele frequencies across the rest of the genome (Fig. S2). As expected, these sequences also revealed that the 100 kb deletion was close to fixation in the SmLE-PZQ-ER population (Fig. S3).

We conducted PZQ dose response curves on these enriched parasite populations. The SmLE-PZQ-ES population had an IC_{50} of 0.198 µg/mL (± 1 s. d.: 0.045), while the SmLE-PZQ-ER population did not reach 50% reduction even at the highest dose (72.9 µg/mL) so has an IC_{50} >72.9 µg/mL: the two purified populations differ by >377-fold in PZQ response (Fig. 4B). These results provide further demonstration that the original SmLE-PZQ-R parasite population was a mixture of PZQ-R and PZQ-S parasites. Separation of the component SmLE-PZQ-ES and SmLE-PZQ-ER parasites from these mixed populations allows rigorous characterization of the PZQ-R trait in parasite populations that are fixed for alternative alleles at *Sm.TRPM$_{PZQ}$*, but contain comparable genomic backgrounds across the rest of the genome.

Sm.TRPM$_{PZQ}$ gene and isoform expression is reduced in SmLE-PZQ-ER parasites

PZQ response varies between parasite stages and sexes, with strongest response in adult males. Adult females and juvenile worms are naturally less susceptible *(30)*. We therefore examined gene expression in the purified SmLE-PZQ-ES and SmLE-PZQ-ER populations (males and females for both adult and juvenile worms) using RNA-seq (Fig. 5). Of the 85 genes expressed in adult worms under the chr. 3 QTL, only the *Sm.TRPM$_{PZQ}$* showed a significant reduction in expression in the SmLE-PZQ-ER adult male

196 worms relative to SmLE-PZQ-ES (2.25-fold, posterior probability = 1) (Fig. 5A-B). Comparable under
197 expression of *Sm.TRPM*$_{PZQ}$ was also seen in female worms when compared to SmLE-PZQ-ES: expression
198 of *Sm.TRPM*$_{PZQ}$ was 11.94-fold lower in female than in male worms, consistent with females being
199 naturally resistant *(30)* (Fig. 5C). However, juvenile male and female worms showed elevated gene
200 expression compared with adult worms (Fig. 5C). This is surprising because juveniles are naturally
201 resistant to PZQ. *Sm.TRPM*$_{PZQ}$ has 41 exons and occurs as 7 isoforms containing between 3 and 36 exons.
202 Strikingly, SmLE-PZQ-ES male worms showed a 4.02-fold higher expression of isoform 6 compared to
203 SmLE-PZQ-ER males, and an 8-fold higher expression than naturally resistant juvenile worms from both
204 populations (while SmLE-PZQ-ER showed only a 2-fold higher expression) (Fig. 5B and D and Fig. S4).
205 This suggests that high expression of isoform 6 is associated with PZQ sensitivity. The 15 exons of
206 isoform 6 produce an 836 amino acid protein that lacks the transmembrane domain but contains the TRP
207 domain. The function of isoform 6 is unclear and we don't know if this association with PZQ sensitivity
208 is causal. We interrogated the 10x single cell expression data from adult worms *(46)* showing that
209 *Sm.TRPM*$_{PZQ}$ is expressed mainly in neural tissue with some expression also in muscle (Fig. S5).

210

211 **Fitness of SmLE-PZQ-ER and SmLE-PZQ-ES parasite populations**

212 Both laboratory selected and field isolated *S. mansoni* showing PZQ-R have been difficult to maintain in
213 the laboratory *(47)*: the PZQ-R trait has been rapidly lost consistent with strong selection against this trait.
214 It has been suggested that PZQ-R carries a fitness cost that will slow spread of this trait in the field under
215 PZQ pressure. Such fitness costs are a common, but not ubiquitous, feature of drug resistance in other
216 pathogens *(48–50)*. We measured several components of parasite fitness in SmLE-PZQ-ES and SmLE-
217 PZQ-ER parasites during laboratory passage of purified parasite lines, but found no significant
218 differences in infectivity to snails, snail survival, or infectivity to hamsters (Fig. S6). We did not see loss
219 of PZQ-R in our lines after 12 generations because the key genome region is fixed. Cioli *et al. (40)* has

also reported long term stability of PZQ-R parasite populations indicative that PZQ-R associated fitness costs maybe limited or absent.

In vivo efficacy of PZQ against SmLE-PZQ-ES and SmLE-PZQ-ER parasites

To determine the relationship between *in vitro* PZQ-R measured in 96-well plates, and *in vivo* resistance, we treated mice infected with either SmLE-PZQ-ER or SmLE-PZQ-ES parasites populations with 120 mg/kg of PZQ. We observed no significant reduction in worm burden in SmLE-PZQ-ER parasites when comparing PZQ-treated and control (DMSO-treated) animals (Wilcoxon test, p = 0.393; Fig. S7A). In contrast, we recovered significantly lower numbers of worms from PZQ-treated versus untreated mice infected with the SmLE-PZQ-ES parasite population (Wilcoxon test, p = 0.008; Fig. S7A). The percent reduction observed was significantly different between the SmLE-PZQ-ES and SmLE-PZQ-ER parasites (Wilcoxon test, p = 0.0129; Fig. S7B). Interestingly, we observed a large reduction in numbers of female worms recovered from PZQ-treated SmLE-PZQ-ES parasites relative to untreated animals (Wilcoxon test, p = 0.008; Fig. S7D), while for male worms this did not reach significance (Wilcoxon test, p = 0.089, Fig. S7C). We saw no impact of PZQ-treatment for either female or male worms in mice infected with SmLE-PZQ-ER. These results show that *in vivo* PZQ response in treated mice differs between SmLE-PZQ-ES and SmLE-PZQ-ER parasites. These data also suggest that the extended paralysis of male SmLE-PZQ-ES worms under PZQ treatment may reduce their ability to maintain female worms *in copula*.

Chemical blockers and activators of *Sm.TRPM$_{PZQ}$* modulate PZQ-R

Sm.TRPM$_{PZQ}$ emerges as a strong candidate gene to explain variation in PZQ response, but validation is required. We were unsuccessful in knocking down expression of *Sm.TRPM$_{PZQ}$* using either siRNA or

dsRNA (Table S2), possibly because this gene is expressed mainly in neural tissue. We therefore used two chemical modulators of Sm.TRPM$_{PZQ}$ activity – an Sm.TRPM$_{PZQ}$ agonist (AG1) and Sm.TRPM$_{PZQ}$ antagonist (ANT1). These were identified among ~16,000 compounds by screening Ca^{2+} influx into HEK293 cells transiently expressing Sm.TRPM$_{PZQ}$ (Chulkov *et al.*, in prep). Addition of the Sm.TRPM$_{PZQ}$ blocker (ANT1) allowed SmLE-PZQ-ES worms to recover from PZQ treatment (Fig. 6A), while the Sm.TRPM$_{PZQ}$ activator (AG1) rendered SmLE-PZQ-ER worms sensitive to PZQ treatment in a dose dependent manner (Fig. 6B). These results are consistent with a role for Sm.TRPM$_{PZQ}$ in determining variation in PZQ response.

We found 5 non-synonymous SNPs and 5 insertions that showed significant differences in allele frequency in *Sm.TRPM$_{PZQ}$* in the SmLE-PZQ-ES and SmLE-PZQ-ER parasite populations. One of these SNPs (*Sm.TRPM$_{PZQ}$*-741903) and two insertions (*Sm.TRPM$_{PZQ}$*-779355 and *Sm.TRPM$_{PZQ}$*-779359) are fixed for alternative alleles in the two populations, with 7 others segregating at different frequencies in the two populations (Fig. S2). These SNPs are located outside the critical transmembrane domains so were not strong candidates to explain differences in PZQ-R. We expressed *Sm.TRPM$_{PZQ}$* carrying some of these variants in HEK293 cells and examined their impact on Ca^{2+} influx to interrogate their role in explaining difference in PZQ response (Fig. S2). None of these SNPs affect Ca^{2+} influx: they are therefore unlikely to underlie PZQ response. We speculate that the difference in PZQ response is due to expression patterns and may be controlled by regulatory variants potentially associated with the adjacent 150 kb deletion or the SOX13 transcription factor.

Sequence variation in *Sm.TRPM$_{PZQ}$* from natural *S. mansoni* populations

Methods for evaluating frequencies of PZQ-resistance mutations in endemic regions would provide a valuable tool for monitoring mass treatment programs aimed at schistosome elimination. Both this paper and the accompanying paper *(21)* identify *Sm.TRPM$_{PZQ}$* as being critical to PZQ-response, and Park *et al*.

have determined critical residues that determine binding between PZQ and *Sm.TRPM*$_{PZQ}$ *(21)*. We examined the mutations present in *Sm.TRPM*$_{PZQ}$ in natural schistosome populations using exome sequencing from 259 miracidia, cercariae or adult parasites from 3 African countries (Senegal, Niger, Tanzania), the Middle East (Oman) and South America (Brazil) *(51, 52)*. We were able to sequence 36/41 exons of *Sm.TRPM*$_{PZQ}$ from 122/259 parasites on average (s.e. = 18.65) (Table S3). We found 1 putative PZQ-R SNP in our reads supported by a very high coverage (Fig. S8). This SNP (c.2708G>T on isoform 5, p.G903*) was found in a single Omani sample and resulted in a truncated protein predicted to result in loss-of-function, demonstrating that PZQ-R alleles are present in natural populations. However, this PZQ-R allele observed was rare and present in heterozygous state so would not impact PZQ response (Fig. S9).

DISCUSSION

Our genetic approach to determining the genes underlying PZQ resistance – using GWAS and a simple lactate-based read out to determine parasite recovery following PZQ treatment in individual parasites – robustly identifies a TRPM channel (*Sm.TRPM*$_{PZQ}$) as the cause of variation in PZQ response. We were further able to purify SmLE-PZQ-ER and SmLE-PZQ-ES parasites to examine drug response and gene expression and to use chemical blockers to directly implicate *Sm.TRPM*$_{PZQ}$. Our results complement those of Park *et al. (21)* who used a pharmacological approach to determine that *Sm.TRPM*$_{PZQ}$ is the major target for PZQ, and identified the critical residues necessary for activation by PZQ. Together, these approaches demonstrate that TRPM is a key determinant of schistosome response to PZQ.

A striking feature of the results is the strength of the PZQ-R phenotype. While previous authors have described quite modest differences (3-5 fold) in PZQ-response among *S. mansoni* isolates *(40)*, this study revealed at least 377-fold difference in IC_{50} between SmLE-PZQ-ER and SmLE-PZQ-ES parasites. These large differences were only evident after we used marker-assisted selection to divide a mixed genotype laboratory *S. mansoni* population into component SmLE-PZQ-ER and SmLE-PZQ-ES populations. The modest IC_{50} differences in previous studies observed are most likely because the parasite lines compared contained mixed populations of both SmLE-PZQ-ER and SmLE-PZQ-ES individuals. This highlights a critical feature of laboratory schistosome populations that is frequently ignored: these populations are genetically variable and contain segregating genetic and phenotypic variation for a wide variety of parasite traits. In this respect they differ from the clonal bacterial or protozoan parasite “strains” used for laboratory research. Importantly, we can use this segregating genetic variation for genetic mapping of biomedically important parasite traits such as PZQ resistance.

There is strong evidence that PZQ-R parasites occur in schistosome populations in the field, but the contribution of PZQ-R to treatment failure in the field are unclear *(53)*. Molecular markers are widely used for monitoring changes in drug resistance mutations in malaria parasites *(54–56)* and for evaluating

benzimidazole resistance in nematode parasites of veterinary importance *(57, 58)*. The discovery of the genetic basis of resistance to another schistosome drug (oxamniquine) *(59)* now makes genetic surveys possible to evaluate oxamniquine resistance in schistosome populations *(52, 60)*. Identification of *Sm.TRPM*$_{PZQ}$ as a critical determinant of PZQ response, and determination of key residues that can underlie PZQ-R, now makes molecular surveillance possible for *S. mansoni*. We examined variation in *Sm.TRPM*$_{PZQ}$ in 259 parasites collected from locations from across the geographical range of this parasite. We were unable to confirm mutations in any of the key residues that block PZQ binding identified in the mutagenesis studies by Park *et al. (21)*. However, we identified a stop codon in a single parasite isolated from a rodent from Oman *(61)* indicating a low frequency of PZQ-R resistance alleles (1/502, frequency = 0.002). This stop codon was in heterozygous state so is unlikely to result in PZQ-R.

These results are extremely encouraging for control programs, but should be viewed with considerable caution for three reasons. First, the regulatory regions determining gene or isoform expression of *Sm.TRPM*$_{PZQ}$ are currently not known, so we were unable to examine regulatory variants of *Sm.TRPM*$_{PZQ}$ in this screen. Such variants could reduce expression of *Sm.TRPM*$_{PZQ}$ resulting in PZQ resistance. We note that coding variants underlying PZQ-R phenotype were not found in our laboratory SmLE-PZQ-ER parasites, suggesting that regulatory changes may underlie this trait. Second, *Sm.TRPM*$_{PZQ}$ is a large gene (120 kb and 41 exons) that is poorly captured by genome sequencing of field samples. We were able to successfully sequence 36/41 exons, including those that directly interact with PZQ *(21)*, using exome capture methods *(51, 52)*. However, improved sequence coverage will be needed for full length sequencing of this gene. Third, the parasite samples we examined did not come from hotspot regions where regular mass drug administration of PZQ has failed to reduce *S. mansoni* burdens *(35, 62)*. Targeted sequencing of miracidia from these populations will be extremely valuable to determine if there are local elevations in *Sm.TRPM*$_{PZQ}$ variants, or if particular variants are enriched in parasites surviving PZQ treatment. Ideally, such sequence surveys should be partnered with functional validation studies in which variant *Sm.TRPM*$_{PZQ}$ are expressed in HEK293 cells to determine their

response to PZQ exposure *(21)*. As the homologous genes in *S. haematobium* and *S. japonicum* are likely to be activated by PZQ, this molecular approach to screening for PZQ resistance should be equally applicable to all major schistosome species infecting humans.

MATERIALS AND METHODS

Study design

This study was designed to determine the genetic basis of PZQ-R, and was stimulated by the initial observation that a laboratory *S. mansoni* population generated through selection with PZQ contained both PZQ-S and PZQ-R individuals. The project had 6 stages: (i) QTL location. We conducted a genome-wide association study (GWAS). This involved measuring the PZQ-response of individual worms, pooling those showing high levels of resistance and low levels of resistance, sequencing the pools to high read depth, and then identifying the genome regions showing significant differences in allele frequencies between high and low resistance parasites. (ii) Fine mapping of candidate genes. We identified potential candidate genes in these QTL regions, through examination of gene annotations, and exclusion of genes that are not expressed in adults. We also determined the mode of inheritance of the PZQ-R locus. (iii) Marker assisted purification of PZQ-S and PZQ-R parasites. To separate PZQ-R and PZQ-S parasites into "pure" populations, we genotyped larval parasites for genetic markers at the PZQ-R locus and infected rodents with genotypes associated with PZQ-R or PZQ-S. We then measured the IC_{50} for each of the purified populations to confirm their PZQ response. (iv) Characterization of purified SmLE-PZQ-ER and SmLE-PZQ-ES populations. Separation of SmLE-PZQ-ES and SmLE-PZQ-ER parasite populations allowed us to characterize these in more detail. Specifically, we measured expression in juvenile and adult worms of both sexes in both populations. We also quantified parasite fitness traits. (v) Functional analysis. We used RNAi and chemical manipulation approaches to modulate activity of candidate genes and determine the impact of PZQ-resistance. We also used transient expression of candidate genes in cultured mammalian cells, to determine the impact of particular SNPs on response to PZQ. (vi) Survey of PZQ-resistance variants in field collected parasites. Having determined the gene underlying PZQ-R in laboratory parasites, we examined sequence variation in this gene in a field collection of *S. mansoni*

parasites to examine the frequency of sequence variants predicted to result in PZQ-resistance. Methods are described in detail (File S1) and in brief below.

Ethics statement

This study was performed following the Guide for the Care and Use of Laboratory Animals of the National Institutes of Health. The protocol was approved by the IACUC of Texas Biomed (permit number: 1419-MA and 1420-MU). Ethical permission for collection of samples from humans are described in Chevalier *et al. (52).*

Biomphalaria glabrata snails and Schistosoma mansoni *parasites*

We used inbred albino *Biomphalaria glabrata* snails (line Bg121 *(63)*). The SmLE parasite population was originally obtained from an infected patient in Brazil *(64)*. The SmLE-PZQ-R schistosome population was generated by applying a single round of PZQ selection pressure on SmLE parasites at both snail and rodent stages *(26)* and has been maintained in our laboratory since 2014.

Drug resistance tests

Dose-response curves to PZQ in SmLE and SmLE-PZQ-R populations

We measured PZQ sensitivity by examining worm motility *(65)* in SmLE and SmLE-PZQ-R parasite populations. Ten adult males from SmLE or SmLE-PZQ-R populations were placed into each well of a 24-well microplate containing DMEM complete media *(59)*. We performed control and experimental groups in triplicate (*N*=240 worms/population). We exposed adult worms to PZQ (0, 0.1 0.3, 0.9, 2.7, 8.1, 24.3 and 72.9 µg/mL) for 24h. Worms were washed (3x) in drug-free medium and incubated (37°C, 5% CO_2) for 2 days. The parasites were observed daily for 5 days and the number of dead worms scored (i.e., opaque worms without movement).

Metabolic assessment of worm viability using L-lactate assay

We adapted a method for metabolic assessment of worm viability using an L-lactate assay *(44)*. SmLE-PZQ-R adult males were individually placed in 96-well plates with filter insert (Millipore) in DMEM complete media. We added PZQ (24.3 µg/mL in DMEM complete media) while controls were treated with the drug diluent DMSO. At 48h post-treatment, the supernatant was collected from each well and immediately stored at -80 °C until processing. We measured L-lactate levels in the supernatants with a colorimetric L-lactate assay kit (Sigma).

Genome wide association analysis and QTL mapping

Schistosome infections

We collected eggs from livers of hamsters infected with SmLE-PZQ-R *(66)* and exposed 1,000 Bg121 snails to 5 miracidia/snail. After 30 days, snails were individually exposed to light to shed cercariae. We exposed 8 hamsters to 840 cercariae (4 cercariae from each snail). We collected adult worms by hamster perfusion 45 days later.

Phenotypic selection

We plated SmLE-PZQ-R adult males individually in 96-well plates in DMEM complete media and treated with a 24.3 µg/mL PZQ. A control group was treated with the drug diluent DMSO. This experiment was done twice independently. A total of 590 and 691 adult males were collected, cultured *in vitro* and exposed to PZQ.

We collected media supernatants in 96-well PCR plates after 24h in culture (pre-treatment) and 48h post-treatment for quantifying L-lactate levels. We took the 20% of the treated worms releasing the highest amount of L-lactate (average L-lactate production ± SD: Experiment 1 = 61.44 nmol/h ± 13.16 / Experiment 2 = 56.38 nmol/h ± 10.82) and the 20% of the treated worms releasing the lowest amount of L-lactate (average L-lactate production ± SD: Experiment 1 = 28.61 nmol/h ± 5.32 / Experiment 2 = 23.04 nmol/h ± 4.14), 48h post PZQ treatment.

DNA extraction and library preparation

We sequenced whole genomes of the two pools of recovered (Experiment 1: 116 worms / Experiment 2: 137 worms) and susceptible worms (Experiment 1: 116 worms / Experiment 2: 137 worms) and measured allele frequencies in each pool to identify genome regions showing high differentiation. We extracted gDNA from pools (Blood and Tissue kit, Qiagen) and prepared whole genome libraries in triplicate (KAPA HyperPlus kit, KAPA Biosystems). Raw sequence data are available at the NCBI Sequence Read Archive (PRJNA699326).

Bioinformatic analysis

We used Jupyter notebook and scripts for processing the sequencing data and identifying the QTL (DOI: 10.5281/zenodo.5297220).

a. ***Sequence analysis and variant calling***

We aligned the sequencing data against the *S. mansoni* reference genome using BWA and SAMtools, used GATK to mark PCR duplicates and recalibrate base scores, the HaplotypeCaller module of GATK to call variants (SNP/indel) and GenotypeGVCFs module to perform joint genotyping. We merged VCF files using the MergeVcfs module. All steps were automated using Snakemake.

b. ***QTL identification***

We examined the difference in allele frequencies between low and high L-lactate parasites across the genome by calculating a *Z*-score at each bi-allelic site, weighed *Z*-scores by including the number of worms in each treatment and the difference in the total read depth across the triplicated libraries of each treatment at the given variant, and combined *Z*-scores generated from each biological replicate. Bonferroni correction was calculated with $\alpha = 0.05$.

Relationship between worm genotype at chr. 2 and 3 and PZQ-R phenotype

We phenotyped and genotyped individual worms to validate the impact of worm genotypes on PZQ resistance phenotype and to determine the mode of inheritance of PZQ-R.

Measuring PZQ-R in individual worms

We plated 120 SmLE-PZQ-R adult males individually in 96-well plates, treated them with PZQ (24.3 µg/mL) and collected media supernatants pre- (24 h) and post- (48 h) treatment, and used L-lactate assays to determine PZQ-R status. gDNA was extracted from each worm individually using Chelex.

PCR-RFLP for chr.2 and chr.3 loci

We designed PCR-RFLP to genotype single worms at loci marking QTL peaks on chr. 2 (C>A, chr SM_V7_2: 1072148) and chr. 3 (T>C, chr SM_V7_3: 741987) (Table S4). To achieve this, we digested PCR amplicons for chr. 2 with BslI and chr. 3 with Mse1, which were visualized by 2% agarose gel electrophoresis.

Quantitative PCR of copy number variation (CNV) in single worms

We genotyped individual worms for a deletion on chr. 3 (position 1220683-1220861 bp) using a qPCR assay. Methods and primers are described in Table S4.

Marker assisted selection of resistant and susceptible parasite populations

Selection of SmLE-PZQ-ER and SmLE-PZQ-ES populations

We separated the polymorphic SmLE-PZQ-R population based on chr. 3 QTL genotype using PCR-RFLP. We exposed 960 Bg121 snails to single SmLE-PZQ-R miracidia *(66)*. We identified infected snails (*N*=272) 4 weeks later, collected cercariae from individual snails, extracted cercarial DNA *(66)*, and genotyped each parasite at the chr. 3 locus (Homozygous R/R: n=89; Homozygous S/S: n=39; Heterozygous R/S: n=117), and determined their gender by PCR *(67)*. We selected 32 R/R parasites and 32 S/S genotypes. For both R/R and S/S we used 13 males and 19 females. We exposed 5 hamsters to 800

454 cercariae of 32 R/R genotypes parasites and 5 hamsters to 800 cercariae 32 S/S genotyped parasites. This
455 single generation marker assisted selection generated two subpopulations: SmLE-PZQ-ER enriched in
456 parasites with R/R genotype, and SmLE-PZQ-ES enriched with S/S genotypes.
457
458 *PZQ IC_{50} with SmLE-PZQ-ER and SmLE-PZQ-ES*
459 Forty-five days after infection, we recovered adult worms of SmLE-PZQ-ER and SmLE-PZQ-ES
460 subpopulations from hamsters. We placed adult males in 96-well plates in DMEM complete media. We
461 determined PZQ dose-response using the same doses as for SmLE-PZQ-R.
462
463 *gDNA extraction and library preparation and bioinformatics*
464 We recovered the F1 SmLE-PZQ-ER and SmLE-PZQ-ES worms and extracted gDNA from pools of
465 adult males or females separately and prepared whole genome libraries from these pools as described
466 above. Sequence data are available at the NCBI Sequence Read Archive (accession numbers
467 PRJNA701978). The analysis was identical to the GWAS and QTL mapping analysis.
468
469 **Transcriptomic analysis of resistant and susceptible schistosome worms at juvenile and adult stages**
470 *Sample collection*
471 We recovered SmLE-PZQ-ER and SmLE-PZQ-ES worms from hamsters at 28 days (juveniles) or 45
472 days (adults) post-infection. For each subpopulation, we collected 3 biological replicates of 30 male or 30
473 female juvenile worms, and 3 biological replicates of 30 males or 60 female adult worms. Different
474 numbers of males and females were used to provide sufficient amount of RNA material for library
475 preparation.
476
477 *RNA extraction and RNA-seq library preparation*
478 ***a. RNA extraction***

We extracted total RNA from juvenile and adult worm pools (RNeasy Mini kit, Qiagen), quantified the RNA recovered (Qubit RNA Assay Kit, Invitrogen) and assessed the RNA integrity by TapeStation (Agilent - RNA integrity numbers: ~8.5–10 for all samples).

b. RNA-seq library preparation

We generated RNA-seq libraries using the KAPA Stranded mRNA-seq kit (KAPA Biosystems) from 500 ng RNA for each library and did 150 bp pair-end sequencing. Raw sequence data are available at the NCBI Sequence Read Archive (accession numbers PRJNA704646).

c. Bioinformatic analysis.

To identify differentially expressed genes, we aligned the sequencing data against the *S. mansoni* reference genome using STAR. We quantified gene and isoform abundances by computing transcripts per million values using RSEM and compared abundances between groups (ES/ER, males/females, juveniles/adults) using the R package EBSeq. Jupyter notebooks and associated scripts are available on Zenodo (DOI: 10.5281/zenodo.5297218)

Manipulation of Sm.TRPM$_{PZQ}$ channel expression or function

RNA interference

We attempted RNA interference to functionally validate the role of *Sm.TRPM$_{PZQ}$* in PZQ resistance. This approach was unsuccessful. Detailed methodology is available in File S1 and Table S2.

Specific Sm.TRPM$_{PZQ}$ chemical inhibitor and activator

We used specific chemical inhibitor and activator (Chulkov *et al.*, in prep) to manipulate the function of Sm.TRPM$_{PZQ}$ to examine the impact on PZQ response. We placed individual SmLE-PZQ-ER and SmLE-PZQ-ES adult males in 96-well plates containing DMEM complete media. After 24h, worms from each population were treated either with a cocktail combining PZQ (1 µg/mL) and the Sm.TRPM$_{PZQ}$ blocker (ANT1 at 50 µM) or the Sm.TRPM$_{PZQ}$ activator (AG1 at 10, 25 or 50 µM) or the drug diluent (DMSO).

We also set up control plates to evaluate the impact of Sm.TRPM$_{PZQ}$ blocker or activator alone. Worms were exposed to these drug cocktails for 24h, washed 3 times with drug-free medium, and incubated (37°C, 5% CO_2) for 2 days. We collected media supernatants before treatment and 48h post-treatment and quantified L-lactate.

In vivo parasite survival after PZQ treatment

We exposed two groups of 12 female Balb/C mice to either SmLE-PZQ-ER or SmLE-PZQ-ES cercariae. Each mouse was infected by tail immersion using 80 cercariae from 40 infected snails. Forty days post-infection, we treated mice by oral gavage with either 120 mg/kg of PZQ (1% DMSO + vegetable oil in a total volume of 150 µL) or the same volume of drug diluent only (control group). We recovered worms 50 days post-infection.

Sm.TRPM$_{PZQ}$ variants in _S. mansoni_ field samples

Variants identification in exome sequence data from natural S. mansoni *parasites*

We utilized *S. mansoni* exome sequence data from Africa, South America and the middle East to investigate variation in *Sm.TRPM$_{PZQ}$*. African miracidia were from the Schistosomiasis collection at the Natural History Museum (SCAN) *(68)*, while Brazilian miracidia and Omani cercariae and adult worms were collected by laboratories at Texas Biomed or University of Perpignan, respectively *(52)*. We have previously described exome sequencing methods for *S. mansoni (51, 52)*. Data were analyzed as described in Chevalier et al. *(52)*. The code is available in Jupyter notebook and associated scripts (DOI: 10.5281/zenodo.5297222).

Sanger re-sequencing to confirm the presence of the Sm.TRPM$_{PZQ}$ *field variants*

To confirm the presence of variants in *Sm.TRPM$_{PZQ}$* when read depth was <10 reads, we performed Sanger re-sequencing of exons of interest *(21)*. Primers and conditions are listed in Table S4. We scored variants using PolyPhred software (v6.18). Sanger traces are available on Zenodo (DOI:

530 10.5281/zenodo.5204523). These analyses are available in the Jupyter notebook and associated scripts
531 (DOI: 10.5281/zenodo.5297222).
532
533 *Functional analysis*
534 We determined whether proteins produced by variant *Sm.TRPM*$_{PZQ}$ alleles were activated by PZQ
535 following Park et al. *(21)*.
536
537 **Statistical analysis**
538 Statistical analyzes and graphs were performed using R software (v3.5.1). We used the drc package from
539 R to analyze dose-response datasets and Readqpcr and Normqpcr packages to analyze RT-qPCR datasets.
540 For non-normal data (Shapiro test, $p < 0.05$), we used Chi-square test or Kruskal-Wallis test followed by
541 pairwise Wilcoxon-Mann-Whitney post-hoc test or a Wilcoxon-Mann-Whitney test. For normal data, we
542 used one–way ANOVA or a pairwise comparison Welsh *t*-test. The confidence intervals were set to 95%
543 and *p*-values < 0.05 were considered significant.
544
545 **Supplementary Materials**
546 Fig. S1. Development of a L-lactate assay for assaying worm recovery.
547 Fig. S2. Validation of marker-assisted selection of SmLE-PZQ-ER and ES using Next Generation
548 Sequencing (NGS).
549 Fig. S3. Large deletions adjacent to *Sm.TRPM*$_{PZQ}$ and SOX13 transcription factor.
550 Fig. S4. Detailed genes and isoforms expression in SmLE-PZQ-ER and SmLE-PZQ-ES parasites.
551 Fig. S5. Cellular localization of *Sm.TRPM*$_{PZQ}$ expression in *S. mansoni*.
552 Fig. S6. Fitness of SmLE-PZQ-ES and SmLE-PZQ-ER parasites.
553 Fig. S7. Impact of *in vivo* PZQ treatment on SmLE-PZQ-ER and SmLE-PZQ-ES parasites.

554 Fig. S8. Stop codon identified in *S. mansoni* field sample from Oman.

555 Fig. S9. *Sm.TRPM*$_{PZQ}$ gene: average exon read depth and identified mutations in field samples.

556 Table S1. Genes in QTL regions on chr. 2 and 3.

557 Table S2. Details of RNAi for *Sm.TRPM*$_{PZQ.}$

558 Table S3. Mutations present in *Sm.TRPM*$_{PZQ}$ in natural schistosome populations from 3 African countries

559 (Senegal, Niger, Tanzania), the Middle East (Oman) and South America (Brazil).

560 Table S4. Summary table of siRNA sequences and primer sequences used for PCR-RFLP, RT-qPCR,

561 PCRs and Sanger sequencing.

562 File S1. Expanded Material and Methods.

563

References and Notes

1. World Health Organization, Schistosomiasis, (available at https://www.who.int/news-room/fact-sheets/detail/schistosomiasis).

2. G. B. D. 2017 Disease, I. Incidence, P. Collaborators, Global, regional, and national incidence, prevalence, and years lived with disability for 354 diseases and injuries for 195 countries and territories, 1990-2017: a systematic analysis for the Global Burden of Disease Study 2017., *Lancet (London, England)* **392**, 1789–1858 (2018).

3. D. P. McManus, D. W. Dunne, M. Sacko, J. Utzinger, B. J. Vennervald, X.-N. Zhou, Schistosomiasis., *Nature reviews. Disease primers* **4**, 13 (2018).

4. G. B. D. 2015 Mortality, C. of Death Collaborators, Global, regional, and national life expectancy, all-cause mortality, and cause-specific mortality for 249 causes of death, 1980-2015: a systematic analysis for the Global Burden of Disease Study 2015., *Lancet (London, England)* **388**, 1459–1544 (2016).

5. M. A. Verjee, Schistosomiasis: Still a cause of significant morbidity and mortality., *Research and reports in tropical medicine* **10**, 153–163 (2019).

6. M. J. van der Werf, S. J. de Vlas, S. Brooker, C. W. N. Looman, N. J. D. Nagelkerke, J. D. F. Habbema, D. Engels, Quantification of clinical morbidity associated with schistosome infection in sub-Saharan Africa., *Acta Trop* **86**, 125–139 (2003).

7. W. H. Organization, others, Schistosomiasis: progress report 2001-2011, strategic plan 2012-2020, (2013).

8. A. K. Deol, F. M. Fleming, B. Calvo-Urbano, M. Walker, V. Bucumi, I. Gnandou, E. M. Tukahebwa, S. Jemu, U. J. Mwingira, A. Alkohlani, M. Traoré, E. Ruberanziza, S. Touré, M.-G. Basáñez, M. D. French, J. P. Webster, Schistosomiasis - assessing progress toward the 2020 and 2025 global goals., *The New England journal of medicine* **381**, 2519–2528 (2019).

9. S. H. Xiao, P. A. Friedman, B. A. Catto, L. T. Webster, Praziquantel-induced vesicle formation in the tegument of male Schistosoma mansoni is calcium dependent., *The Journal of parasitology* **70**, 177–179 (1984).

10. R. Pax, J. L. Bennett, R. Fetterer, A benzodiazepine derivative and praziquantel: effects on musculature of Schistosoma mansoni and Schistosoma japonicum., *Naunyn-Schmiedeberg's archives of pharmacology* **304**, 309–315 (1978).

11. B. Becker, H. Mehlhorn, P. Andrews, H. Thomas, J. Eckert, Light and electron microscopic studies on the effect of praziquantel on Schistosoma mansoni, Dicrocoelium dendriticum, and Fasciola hepatica (Trematoda) in vitro., *Zeitschrift fur Parasitenkunde (Berlin, Germany)* **63**, 113–128 (1980).

12. C. S. Bricker, J. W. Depenbusch, J. L. Bennett, D. P. Thompson, The relationship between tegumental disruption and muscle contraction in Schistosoma mansoni exposed to various compounds., *Zeitschrift fur Parasitenkunde (Berlin, Germany)* **69**, 61–71 (1983).

13. P. M. Cupit, C. Cunningham, What is the mechanism of action of praziquantel and how might resistance strike?, *Future medicinal chemistry* **7**, 701–705 (2015).

14. C. M. Thomas, D. J. Timson, The mechanism of action of praziquantel: Six hypotheses., *Current topics in medicinal chemistry* **18**, 1575–1584 (2018).

15. A. B. Kohn, P. A. Anderson, J. M. Roberts-Misterly, R. M. Greenberg, Schistosome calcium channel beta subunits. Unusual modulatory effects and potential role in the action of the antischistosomal drug praziquantel., *The Journal of biological chemistry* **276**, 36873–36876 (2001).

16. M. C. Jeziorski, R. M. Greenberg, Voltage-gated calcium channel subunits from platyhelminths: potential role in praziquantel action., *International journal for parasitology* **36**, 625–632 (2006).

17. J. D. Chan, M. Zarowiecki, J. S. Marchant, Ca^{2+} channels and praziquantel: a view from the free world., *Parasitology international* **62**, 619–628 (2013).

18. R. S. Kasinathan, L. K. Sharma, C. Cunningham, T. R. Webb, R. M. Greenberg, Inhibition or knockdown of ABC transporters enhances susceptibility of adult and juvenile schistosomes to Praziquantel., *PLoS neglected tropical diseases* **8**, e3265 (2014).

19. R. M. Greenberg, ABC multidrug transporters in schistosomes and other parasitic flatworms., *Parasitology international* **62**, 647–653 (2013).

20. S.-K. Park, G. S. Gunaratne, E. G. Chulkov, F. Moehring, P. McCusker, P. I. Dosa, J. D. Chan, C. L. Stucky, J. S. Marchant, The anthelmintic drug praziquantel activates a schistosome transient receptor potential channel., *The Journal of biological chemistry* **294**, 18873–18880 (2019).

21. S.-K. Park, L. Friedrich, N. A. Yahya, C. Rohr, E. G. Chulkov, D. Maillard, F. Rippmann, T. Spangenberg, J. S. Marchant, Mechanism of praziquantel action at a parasitic flatworm ion channel, *bioRxiv* (2021), doi:10.1101/2021.03.09.434291.

22. P. G. Fallon, M. J. Doenhoff, Drug-resistant schistosomiasis: resistance to praziquantel and oxamniquine induced in *Schistosoma mansoni* in mice is drug specific., *Am J Trop Med Hyg* **51**, 83–88 (1994).

23. B. Gryseels, L. Nkulikyinka, D. Engels, Impact of repeated community-based selective chemotherapy on morbidity due to schistosomiasis mansoni., *The American journal of tropical medicine and hygiene* **51**, 634–641 (1994).

24. M. Ismail, S. Botros, A. Metwally, S. William, A. Farghally, L. F. Tao, T. A. Day, J. L. Bennett, Resistance to praziquantel: direct evidence from Schistosoma mansoni isolated from Egyptian villagers., *The American journal of tropical medicine and hygiene* **60**, 932–935 (1999).

25. D. Alonso, J. Muñoz, J. Gascón, M. E. Valls, M. Corachan, Failure of standard treatment with praziquantel in two returned travelers with Schistosoma haematobium infection., *The American journal of tropical medicine and hygiene* **74**, 342–344 (2006).

26. F. F. B. Couto, P. M. Z. Coelho, N. Araújo, J. R. Kusel, N. Katz, L. K. Jannotti-Passos, A. C. A. Mattos, Schistosoma mansoni: a method for inducing resistance to praziquantel using infected Biomphalaria glabrata snails., *Memorias do Instituto Oswaldo Cruz* **106**, 153–157 (2011).

27. W. Wang, L. Wang, Y.-S. Liang, Susceptibility or resistance of praziquantel in human schistosomiasis: a review., *Parasitology research* **111**, 1871–1877 (2012).

28. L. Pica-Mattoccia, M. J. Doenhoff, C. Valle, A. Basso, A.-R. Troiani, P. Liberti, A. Festucci, A. Guidi, D. Cioli, Genetic analysis of decreased praziquantel sensitivity in a laboratory strain of *Schistosoma mansoni*., *Acta Trop* **111**, 82–85 (2009).

29. J. Zwang, P. Olliaro, Efficacy and safety of praziquantel 40 mg/kg in preschool-aged and school-aged children: a meta-analysis., *Parasites & vectors* **10**, 47 (2017).

30. L. Pica-Mattoccia, D. Cioli, Sex- and stage-related sensitivity of Schistosoma mansoni to in vivo and in vitro praziquantel treatment., *International journal for parasitology* **34**, 527–533 (2004).

31. S. Botros, L. Pica-Mattoccia, S. William, N. El-Lakkani, D. Cioli, Effect of praziquantel on the immature stages of Schistosoma haematobium., *International journal for parasitology* **35**, 1453–1457 (2005).

643 32. M. Ismail, A. Metwally, A. Farghaly, J. Bruce, L. F. Tao, J. L. Bennett, Characterization of isolates of
644 Schistosoma mansoni from Egyptian villagers that tolerate high doses of praziquantel., *The American journal of*
645 *tropical medicine and hygiene* **55**, 214–218 (1996).

646 33. S. D. Melman, M. L. Steinauer, C. Cunningham, L. S. Kubatko, I. N. Mwangi, N. B. Wynn, M. W. Mutuku, D.
647 M. S. Karanja, D. G. Colley, C. L. Black, W. E. Secor, G. M. Mkoji, E. S. Loker, Reduced susceptibility to
648 praziquantel among naturally occurring Kenyan isolates of Schistosoma mansoni., *PLoS neglected tropical diseases*
649 **3**, e504 (2009).

650 34. S. William, S. Botros, M. Ismail, A. Farghally, T. A. Day, J. L. Bennett, Praziquantel-induced tegumental
651 damage in vitro is diminished in schistosomes derived from praziquantel-resistant infections., *Parasitology* **122 Pt 1**,
652 63–66 (2001).

653 35. N. Kittur, C. H. Campbell, S. Binder, Y. Shen, R. E. Wiegand, J. R. Mwanga, S. M. Kinung'hi, R. M. Musuva,
654 M. R. Odiere, S. H. Matendechero, S. Knopp, D. G. Colley, Discovering, defining, and summarizing persistent
655 hotspots in SCORE studies., *The American journal of tropical medicine and hygiene* **103**, 24–29 (2020).

656 36. P. A. Mawa, J. Kincaid-Smith, E. M. Tukahebwa, J. P. Webster, S. Wilson, Schistosomiasis morbidity hotspots:
657 Roles of the human host, the parasite and their interface in the development of severe morbidity., *Frontiers in*
658 *immunology* **12**, 635869 (2021).

659 37. T. Crellen, M. Walker, P. H. L. Lamberton, N. B. Kabatereine, E. M. Tukahebwa, J. A. Cotton, J. P. Webster,
660 Reduced efficacy of praziquantel against schistosoma mansoni is associated with multiple rounds of mass drug
661 administration., *Clinical infectious diseases : an official publication of the Infectious Diseases Society of America*
662 **63**, 1151–1159 (2016).

663 38. A. V. Protasio, I. J. Tsai, A. Babbage, S. Nichol, M. Hunt, M. A. Aslett, N. De Silva, G. S. Velarde, T. J. C.
664 Anderson, R. C. Clark, C. Davidson, G. P. Dillon, N. E. Holroyd, P. T. LoVerde, C. Lloyd, J. McQuillan, G.
665 Oliveira, T. D. Otto, S. J. Parker-Manuel, M. A. Quail, R. A. Wilson, A. Zerlotini, D. W. Dunne, M. Berriman, A
666 systematically improved high quality genome and transcriptome of the human blood fluke *Schistosoma mansoni*.,
667 *PLoS Negl Trop Dis* **6**, e1455 (2012).

668 39. T. J. C. Anderson, P. T. LoVerde, W. Le Clec'h, F. D. Chevalier, Genetic crosses and linkage mapping in
669 schistosome parasites., *Trends Parasitol* **34**, 982–996 (2018).

670 40. D. Cioli, S. S. Botros, K. Wheatcroft-Francklow, A. Mbaye, V. Southgate, L.-A. T. Tchuenté, L. Pica-Mattoccia,
671 A. R. Troiani, S. H. S. El-Din, A.-N. A. Sabra, J. Albin, D. Engels, M. J. Doenhoff, Determination of ED50 values
672 for praziquantel in praziquantel-resistant and -susceptible Schistosoma mansoni isolates., *International journal for*
673 *parasitology* **34**, 979–987 (2004).

674 41. S. K. Volkman, J. Herman, A. K. Lukens, D. L. Hartl, Genome-wide association studies of drug-resistance
675 determinants., *Trends in parasitology* **33**, 214–230 (2017).

676 42. J. Wit, C. M. Dilks, E. C. Andersen, Complementary approaches with free-living and parasitic nematodes to
677 understanding anthelmintic resistance., *Trends in parasitology* **37**, 240–250 (2021).

678 43. R. H. Fetterer, R. A. Pax, J. L. Bennett, Praziquantel, potassium and 2,4-dinitrophenol: analysis of their action
679 on the musculature of Schistosoma mansoni., *European journal of pharmacology* **64**, 31–38 (1980).

680 44. S. Howe, D. Zöphel, H. Subbaraman, C. Unger, J. Held, T. Engleitner, W. H. Hoffmann, A. Kreidenweiss,
681 Lactate as a novel quantitative measure of viability in Schistosoma mansoni drug sensitivity assays., *Antimicrobial*
682 *agents and chemotherapy* **59**, 1193–1199 (2015).

683 45. M. Girardot, E. Bayet, J. Maurin, P. Fort, P. Roux, P. Raynaud, SOX9 has distinct regulatory roles in alternative
684 splicing and transcription., *Nucleic acids research* **46**, 9106–9118 (2018).

685 46. G. Wendt, L. Zhao, R. Chen, C. Liu, A. J. O'Donoghue, C. R. Caffrey, M. L. Reese, J. J. Collins, A single-cell
686 RNA-seq atlas of , javax.xml.bind.JAXBElement@463bbb2c, identifies a key regulator of blood feeding., *Science*
687 *(New York, N.Y.)* **369**, 1644–1649 (2020).

688 47. S. William, A. Sabra, F. Ramzy, M. Mousa, Z. Demerdash, J. L. Bennett, T. A. Day, S. Botros, Stability and
689 reproductive fitness of Schistosoma mansoni isolates with decreased sensitivity to praziquantel., *International*
690 *journal for parasitology* **31**, 1093–1100 (2001).

691 48. S. Hernando-Amado, F. Sanz-García, P. Blanco, J. L. Martínez, Fitness costs associated with the acquisition of
692 antibiotic resistance., *Essays in biochemistry* **61**, 37–48 (2017).

693 49. P. Durão, R. Balbontín, I. Gordo, Evolutionary mechanisms shaping the maintenance of antibiotic resistance.,
694 *Trends in microbiology* **26**, 677–691 (2018).

695 50. S. Nair, X. Li, G. A. Arya, M. McDew-White, M. Ferrari, F. Nosten, T. J. C. Anderson, Fitness costs and the
696 rapid spread of , javax.xml.bind.JAXBElement@527e161e, -C580Y substitutions conferring artemisinin resistance.,
697 *Antimicrobial agents and chemotherapy* **62** (2018), doi:10.1128/AAC.00605-18.

698 51. W. Le Clec'h, F. D. Chevalier, M. McDew-White, F. Allan, B. L. Webster, A. N. Gouvras, S. Kinunghi, L.-A.
699 Tchuem Tchuenté, A. Garba, K. A. Mohammed, S. M. Ame, J. P. Webster, D. Rollinson, A. M. Emery, T. J. C.
700 Anderson, Whole genome amplification and exome sequencing of archived schistosome miracidia., *Parasitology*
701 **145**, 1739–1747 (2018).

702 52. F. D. Chevalier, W. Le Clec'h, M. McDew-White, V. Menon, M. A. Guzman, S. P. Holloway, X. Cao, A. B.
703 Taylor, S. Kinung'hi, A. N. Gouvras, B. L. Webster, J. P. Webster, A. M. Emery, D. Rollinson, A. Garba Djirmay,
704 K. M. Al Mashikhi, S. Al Yafae, M. A. Idris, H. Moné, G. Mouahid, P. J. Hart, P. T. LoVerde, T. J. C. Anderson,
705 Oxamniquine resistance alleles are widespread in Old World Schistosoma mansoni and predate drug deployment.,
706 *PLoS pathogens* **15**, e1007881 (2019).

707 53. D. J. Berger, T. Crellen, P. H. L. Lamberton, F. Allan, A. Tracey, J. D. Noonan, N. B. Kabatereine, E. M.
708 Tukahebwa, M. Adriko, N. Holroyd, J. P. Webster, M. Berriman, J. A. Cotton, Whole-genome sequencing of
709 \emphSchistosoma mansoni reveals extensive diversity with limited selection despite mass drug administration,
710 *Nature communications* **12** (2021), doi:10.1038/s41467-021-24958-0.

711 54. D. Ménard, N. Khim, J. Beghain, A. A. Adegnika, M. Shafiul-Alam, O. Amodu, G. Rahim-Awab, C. Barnadas,
712 A. Berry, Y. Boum, M. D. Bustos, J. Cao, J.-H. Chen, L. Collet, L. Cui, G.-D. Thakur, A. Dieye, D. Djallé, M. A.
713 Dorkenoo, C. E. Eboumbou-Moukoko, F.-E.-C. J. Espino, T. Fandeur, M.-F. Ferreira-da-Cruz, A. A. Fola, H.-P.
714 Fuehrer, A. M. Hassan, S. Herrera, B. Hongvanthong, S. Houzé, M. L. Ibrahim, M. Jahirul-Karim, L. Jiang, S.
715 Kano, W. Ali-Khan, M. Khanthavong, P. G. Kremsner, M. Lacerda, R. Leang, M. Leelawong, M. Li, K. Lin, J.-B.
716 Mazarati, S. Ménard, I. Morlais, H. Muhindo-Mavoko, L. Musset, K. Na-Bangchang, M. Nambozi, K. Niaré, H.
717 Noedl, J.-B. Ouédraogo, D. R. Pillai, B. Pradines, B. Quang-Phuc, M. Ramharter, M. Randrianarivelojosia, J.
718 Sattabongkot, A. Sheikh-Omar, K. D. Silué, S. B. Sirima, C. Sutherland, D. Syafruddin, R. Tahar, L.-H. Tang, O. A.
719 Touré, P. Tshibangu-wa-Tshibangu, I. Vigan-Womas, M. Warsame, L. Wini, S. Zakeri, S. Kim, R. Eam, L. Berne,
720 C. Khean, S. Chy, M. Ken, K. Loch, L. Canier, V. Duru, E. Legrand, J.-C. Barale, B. Stokes, J. Straimer, B.
721 Witkowski, D. A. Fidock, C. Rogier, P. Ringwald, F. Ariey, O. Mercereau-Puijalon, K. A. R. M. A. Consortium, A
722 worldwide map of plasmodium falciparum k13-propeller polymorphisms., *The New England journal of medicine*
723 **374**, 2453–2464 (2016).

724 55. M. Mayxay, S. Nair, D. Sudimack, M. Imwong, N. Tanomsing, T. Pongvongsa, S. Phompida, R. Phetsouvanh,
725 N. J. White, T. J. C. Anderson, P. N. Newton, Combined molecular and clinical assessment of Plasmodium
726 falciparum antimalarial drug resistance in the Lao People's Democratic Republic (Laos)., *The American journal of*
727 *tropical medicine and hygiene* **77**, 36–43 (2007).

728 56. T. O. Apinjoh, A. Ouattara, V. P. K. Titanji, A. Djimde, A. Amambua-Ngwa, Genetic diversity and drug
729 resistance surveillance of Plasmodium falciparum for malaria elimination: is there an ideal tool for resource-limited
730 sub-Saharan Africa?, *Malaria journal* **18**, 217 (2019).

731 57. A. C. Kotze, R. K. Prichard, Anthelmintic resistance in haemonchus contortus: History, mechanisms and
732 diagnosis., *Advances in parasitology* **93**, 397–428 (2016).

733 58. L. A. Melville, E. Redman, A. A. Morrison, P. C. Rebecca Chen, R. Avramenko, S. Mitchell, J. Van Dijk, G.
734 Innocent, F. Sargison, C. Aitken, J. S. Gilleard, D. J. Bartley, Large scale screening for benzimidazole resistance
735 mutations in Nematodirus battus, using both pyrosequence genotyping and deep amplicon sequencing, indicates the
736 early emergence of resistance on UK sheep farms., *International journal for parasitology. Drugs and drug*
737 *resistance* **12**, 68–76 (2020).

738 59. C. L. L. Valentim, D. Cioli, F. D. Chevalier, X. Cao, A. B. Taylor, S. P. Holloway, L. Pica-Mattoccia, A. Guidi,
739 A. Basso, I. J. Tsai, M. Berriman, C. Carvalho-Queiroz, M. Almeida, H. Aguilar, D. E. Frantz, P. J. Hart, P. T.
740 LoVerde, T. J. C. Anderson, Genetic and molecular basis of drug resistance and species-specific drug action in
741 schistosome parasites., *Science (New York, N.Y.)* **342**, 1385–1389 (2013).

742 60. F. D. Chevalier, W. Le Clec'h, N. Eng, A. R. Rugel, R. R. de Assis, G. Oliveira, S. P. Holloway, X. Cao, P. J.
743 Hart, P. T. LoVerde, T. J. C. Anderson, Independent origins of loss-of-function mutations conferring oxamniquine
744 resistance in a Brazilian schistosome population., *International journal for parasitology* **46**, 417–424 (2016).

745 61. G. Mouahid, M. A. Idris, O. Verneau, A. Théron, M. M. A. Shaban, H. Moné, A new chronotype of
746 \emphSchistosoma mansoni: adaptive significance., *Trop Med Int Health* **17**, 727–732 (2012).

747 62. R. K. Assaré, R. N. N'Tamon, L. G. Bellai, J. A. Koffi, T.-B. I. Mathieu, M. Ouattara, E. Hürlimann, J. T.
748 Coulibaly, S. Diabaté, E. K. N'Goran, J. Utzinger, Characteristics of persistent hotspots of Schistosoma mansoni in
749 western Côte d'Ivoire., *Parasites & vectors* **13**, 337 (2020).

750 63. K. M. Bonner, C. J. Bayne, M. K. Larson, M. S. Blouin, Effects of Cu/Zn superoxide dismutase (SOD1)
751 genotype and genetic background on growth, reproduction and defense in *Biomphalaria glabrata*., *PLoS Negl Trop*
752 *Dis* **6**, e1701 (2012).

753 64. F. A. Lewis, M. A. Stirewalt, C. P. Souza, G. Gazzinelli, Large-scale laboratory maintenance of *Schistosoma*
754 *mansoni*, with observations on three schistosome/snail host combinations., *J Parasitol* **72**, 813–829 (1986).

755 65. D. Cioli, L. Pica-Mattoccia, R. Moroni, Schistosoma mansoni: hycanthone/oxamniquine resistance is controlled
756 by a single autosomal recessive gene., *Experimental parasitology* **75**, 425–432 (1992).

757 66. W. Le Clec'h, R. Diaz, F. D. Chevalier, M. McDew-White, T. J. C. Anderson, Striking differences in virulence,
758 transmission and sporocyst growth dynamics between two schistosome populations., *Parasites & vectors* **12**, 485
759 (2019).

760 67. F. D. Chevalier, W. Le Clec'h, A. C. Alves de Mattos, P. T. LoVerde, T. J. C. Anderson, Real-time PCR for
761 sexing Schistosoma mansoni cercariae., *Mol Biochem Parasitol* **205**, 35–38 (2016).

762 68. A. M. Emery, F. E. Allan, M. E. Rabone, D. Rollinson, Schistosomiasis collection at NHM (SCAN)., *Parasites*
763 *& vectors* **5**, 185 (2012).

764 69. R. H. Duvall, W. B. DeWitt, An improved perfusion technique for recovering adult schistosomes from
765 laboratory animals., *The American journal of tropical medicine and hygiene* **16**, 483–486 (1967).

766 70. G. Krautz-Peterson, R. Bhardwaj, Z. Faghiri, C. A. Tararam, P. J. Skelly, RNA interference in schistosomes:
767 machinery and methodology., *Parasitology* **137**, 485–495 (2010).

768 71. J. Wang, C. Paz, G. Padalino, A. Coghlan, Z. Lu, I. Gradinaru, J. N. R. Collins, M. Berriman, K. F. Hoffmann, J.
769 J. Collins, Large-scale RNAi screening uncovers therapeutic targets in the parasite \emphSchistosoma mansoni,
770 *Science (New York, N.Y.)* **369**, 1649–1653 (2020).

771 72. X. Rao, X. Huang, Z. Zhou, X. Lin, An improvement of the 2ˆ(-delta delta CT) method for quantitative real-time
772 polymerase chain reaction data analysis., *Biostatistics, bioinformatics and biomathematics* **3**, 71–85 (2013).

773

774 **Acknowledgments:** We thank the Vivarium of the Southwest National Primate Research Center
775 (SNPRC) for providing rodent care. This research was supported by a Cowles fellowship (WLC) from
776 Texas Biomedical Research Institute (13-1328.021), and NIH R01AI133749 (TJCA) and was conducted
777 in facilities constructed with support from Research Facilities Improvement Program grant C06
778 RR013556 from the National Center for Research Resources. SNPRC research at Texas Biomedical
779 Research Institute is supported by grant P51 OD011133 from the 570 Office of Research Infrastructure
780 Programs, NIH. Miracidia samples for sequence analysis were provided by Schistosomiasis Collection at
781 the Natural History Museum (SCAN) funded by the Wellcome Trust (grant 104958/Z/14/Z) and curated
782 by Muriel Rabone. We thank Dr Oumar T. Diaw and Moumoudane M. Seye (Institut Sénégalais de
783 Recherches Agricoles, Senegal) for the collections in Senegal (EU-CONTRAST project); Dr Anouk
784 Gouvras (Global Schistosomiasis Alliance (GSA)), Mariama Lamine and the Re´seau International
785 Schistosomiases Environnemental Aménagement et Lutte (RISEAL) team (Niger) for the collections in
786 Niger; Dr Anouk Gouvras (GSA) and the National Institute for Medical Research (NIMR, Mwanza
787 Tanzania) team Dr Teckla Angelo, Honest Nagai, Boniface Emmanuel, John Igogote, Sarah Buddenborg
788 and Reuben Jonathan for the collections in Tanzania as part of the Schistosomiasis Consortium for
789 Operational Research and Evaluation (SCORE) project (https://score.uga.edu).

790 **Funding:**

791 National Institutes of Health grant 1R01AI123434 (TJCA, PTL)

792 National Institutes of Health grant 1R01AI133749 (TJCA)

793 National Institutes of Health grant NIH R01AI145871 (JSM)

794 Ministry of Health in Oman, the Sultan Qaboos University (grant no. IG/ MED/MICR/00/01)
795 French Ministry of Foreign Affairs (French Embassy in Oman) (grants nos. 402419B, 402415K
796 and 339660F)
797 CNRS- Sciences de la Vie (grants no. 01N92/0745/1 and 02N60/1340)
798 CNRS-Direction des Relations internationales (grants no. 01N92/0745 and 02N60/1340)
799 PICS-CNRS no. 06249: FRANC-INCENSE

800 **Author contributions:**

801 Conceptualization: WLC, PTL, TJCA
802 Methodology: WLC, FDC, PTL, JM
803 Investigation: WLC, FDC, ACM, AS, RD, JM
804 Visualization: WLC, FDC
805 Field samples: HM, GM, MI, KAM, SAY
806 Funding acquisition: TJCA, PTL, JM, HM, GM
807 Project administration: TJCA, PTL
808 Supervision: TJCA, WLC, FDC, PTL, JM
809 Writing – original draft: TJCA, WLC, FDC
810 Writing – review & editing: TJCA, WLC, FDC, PTL, JM, HM, GM

811 **Competing interests:** Authors declare that they have no competing interests.

812 **Data and materials availability:**

813 Phenotype, genotype and fitness data are available from: Zenodo – DOI: 10.5281/zenodo.5209300

814 Sequence data is available from: PRJNA699326, PRJNA701978, PRJNA704646

815 Sequence data from field collected *S. mansoni* is available from: PRJNA439266, PRJNA560070,
816 PRJNA560069, PRJNA743359

817 Code is available on Zenodo (DOIs: 10.5281/zenodo.5297220, 10.5281/zenodo.5297218,

818 10.5281/zenodo.5297222)

819

FIGURES LEGENDS

Fig. 1. Dose response curves for SmLE (PZQ-S) and the derived SmLE-PZQ-R (PZQ-R) populations. PZQ dose response curves show a ~14-fold difference in response between SmLE (ancestral population) and SmLE-PZQ-R (PZQ selected population) (χ^2 test = 10.387, p = 0.001). The PZQ-selected laboratory schistosome population (SmLE-PZQ-R) is polymorphic for drug response. 35% of SmLE-PZQ-R are not killed by treatment with high dose of PZQ, suggesting that this population is polymorphic (*N*=240 worms/populations).

Fig. 2. Genome-wide association mapping of PZQ response. **(A)** We measured recovery of individual adult male worms following expose to 24 µg/mL PZQ by measuring L-lactate production. The distribution from both experimental replicates is shown (A: *N*=590; B: *N*=691). Worms in the bottom (teal) and top (gold) quintile were each pooled, and genome sequenced to high read depth. **(B)** The Manhattan plot identifies genome regions that differ in allele frequency between high and low L-lactate worm pools. Blue dotted line refers to the Bonferroni significance threshold; red dots represent association of individual SNPs; orange arrows mark the position of prominent QTLs. **(C)** The chr. 3 QTL identified spans 4 Mb and 91 genes. Boxes under the Manhattan plot show gene locations (black = expressed, grey = unexpressed). Position of the Sm.TRPM$_{PZQ}$ is marked with dashed lines.

Fig. 3. Inheritance of PZQ response in LE-PZQ population. Bar charts show the change in L-lactate production after exposure to 24 µg/mL PZQ in worms from different genotypic classes for QTL regions on chr. 2 and 3. **(A)** chr. 2 QTL (Kruskal-Wallis KW test χ^2 = 0.019, p = 0.99), **(B)** *Sm.TRPM$_{PZQ}$*-741987C (KW test χ^2 = 24.481, p = 2.93x10^{-6}), **(C)** 100kb deletion (KW test χ^2 = 15.708, p = 0.0004). We see minimal change in L-lactate production following PZQ exposure in homozygotes for the SNP enriched in PZQ treated parasites, indicating that this trait is recessive. Parasites carrying two copies of

844 the 100 kb deletion are also strongly associated with resistance, demonstrating that this deletion is in LD
845 (N = 120 worms; NS: No significant difference between groups; *$p < 0.05$; ** $p \leq 0.01$; *** $p \leq 0.001$).

846

847 **Fig. 4. Single generation marker-assisted purification of SmLE-PZQ-ES and SmLE-PZQ-ER**
848 **parasites. (A)** Experimental strategy for identifying parasite larvae that are homozygous for *Sm.TRPM$_{PZQ}$*
849 alleles associated with PZQ-R or PZQ-S. We genotyped cercaria larvae emerging from snails infected
850 with single parasite genotypes for a restriction site in the *Sm.TRPM$_{PZQ}$* gene, and then infected two groups
851 of hamsters with parasites homozygous for alternative alleles at this locus. **(B)** The two populations of
852 parasites generated show dramatic differences in PZQ-response (N = 60 worms/population/treatment, χ^2
853 test = 373.03, $p < 2.2x10^{-16}$).

854

855 **Fig. 5. Gene expression differences between SmLE-PZQ-ES and SmLE-PZQ-ER parasites.** Volcano
856 plot showing the differential **(A)** gene expression and **(B)** isoform expression between adult male PZQ-ES
857 and PZQ-ER (in black: genes or isoforms showing significant differential expression genome-wide, in
858 blue: genes or isoforms located under the chr. 3 QTL, in red: *Sm.TRPM$_{PZQ}$* gene or isoform). **(C)**
859 *Sm.TRPM$_{PZQ}$* gene expression and **(D)** *Sm.TRPM$_{PZQ}$* isoform 6 expression level comparison between PZQ-
860 ES and ER for the two sex (i.e. male and females) and different stages (i.e. adult and juvenile). High
861 expression of *Sm.TRPM$_{PZQ}$* isoform 6 is associated with PZQ sensitivity.

862

863 **Fig. 6. Impact of *Sm.TRPM$_{PZQ}$* blockers and activators on PZQ response. (A)** SmLE-PZQ-ES and **(B)**
864 SmLE-PZQ-ER were exposed to either i) PZQ or DMSO alone (control group), ii) PZQ or DMSO
865 combined with 50 µM Sm.TRPM$_{PZQ}$ blocker (antagonist ANT1), iii) PZQ or DMSO combined with
866 either 10 µM, 25 µM or 50 µM of Sm.TRPM$_{PZQ}$ activator (agonist AG1). Parasite viability was assessed 3

867 days post-treatment, based on their L-lactate production. Addition of the Sm.TRPM$_{PZQ}$ blocker allowed
868 SmLE-PZQ-ES worms to recover from PZQ treatment (Welsh t-test, t = -0.94, p = 0.35), while the
869 Sm.TRPM$_{PZQ}$ activator (agonist AG1) rendered SmLE-PZQ-ER worms sensitive to PZQ treatment in a
870 dose dependent manner (N = 20 worms/population/treatment; Welsh t-test, NS: No significant difference
871 between groups; *$p < 0.05$; ** $p \leq 0.01$; *** $p \leq 0.001$.)

872 **Fig. 1**

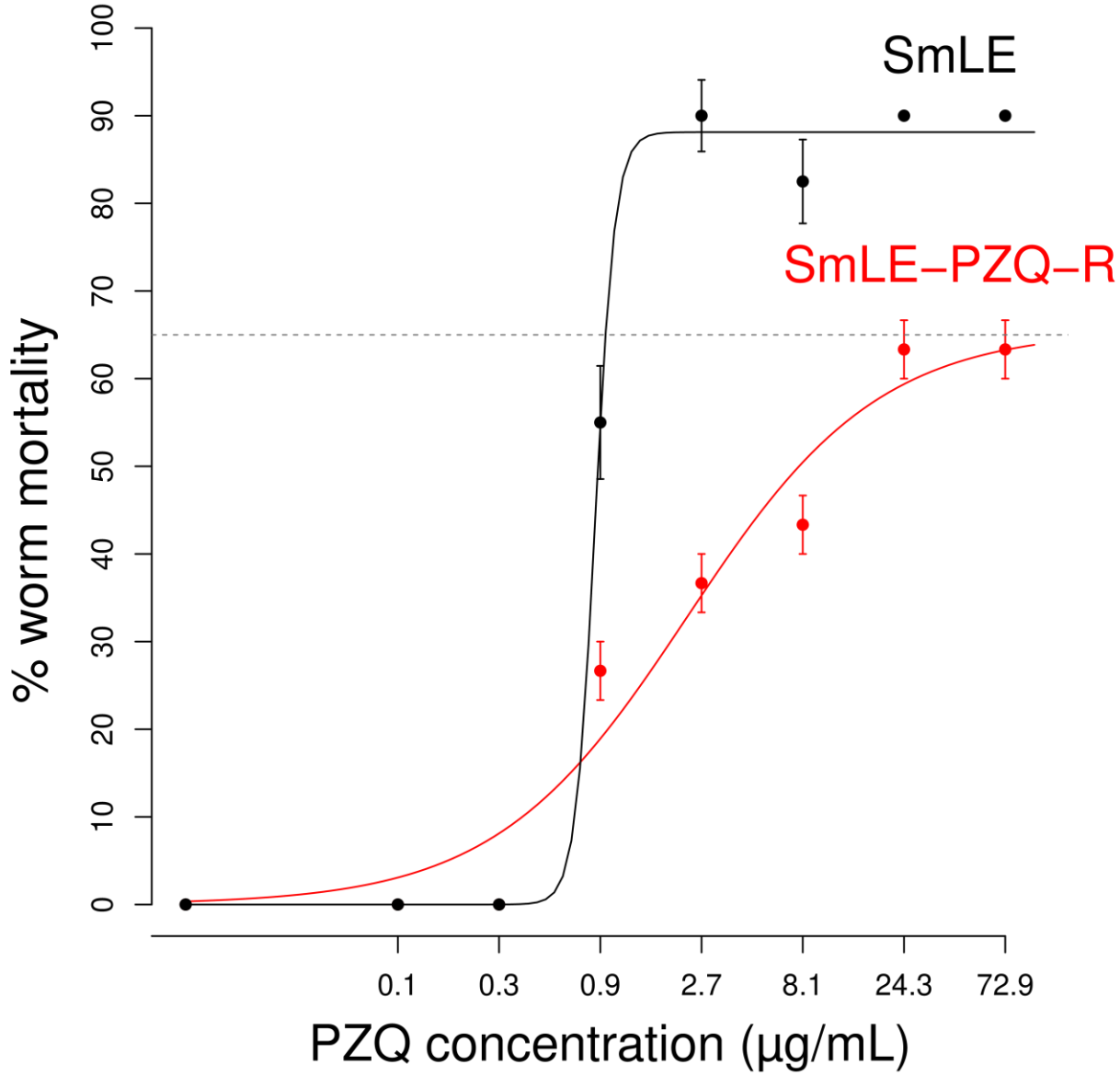

873

874

875 **Fig. 2**

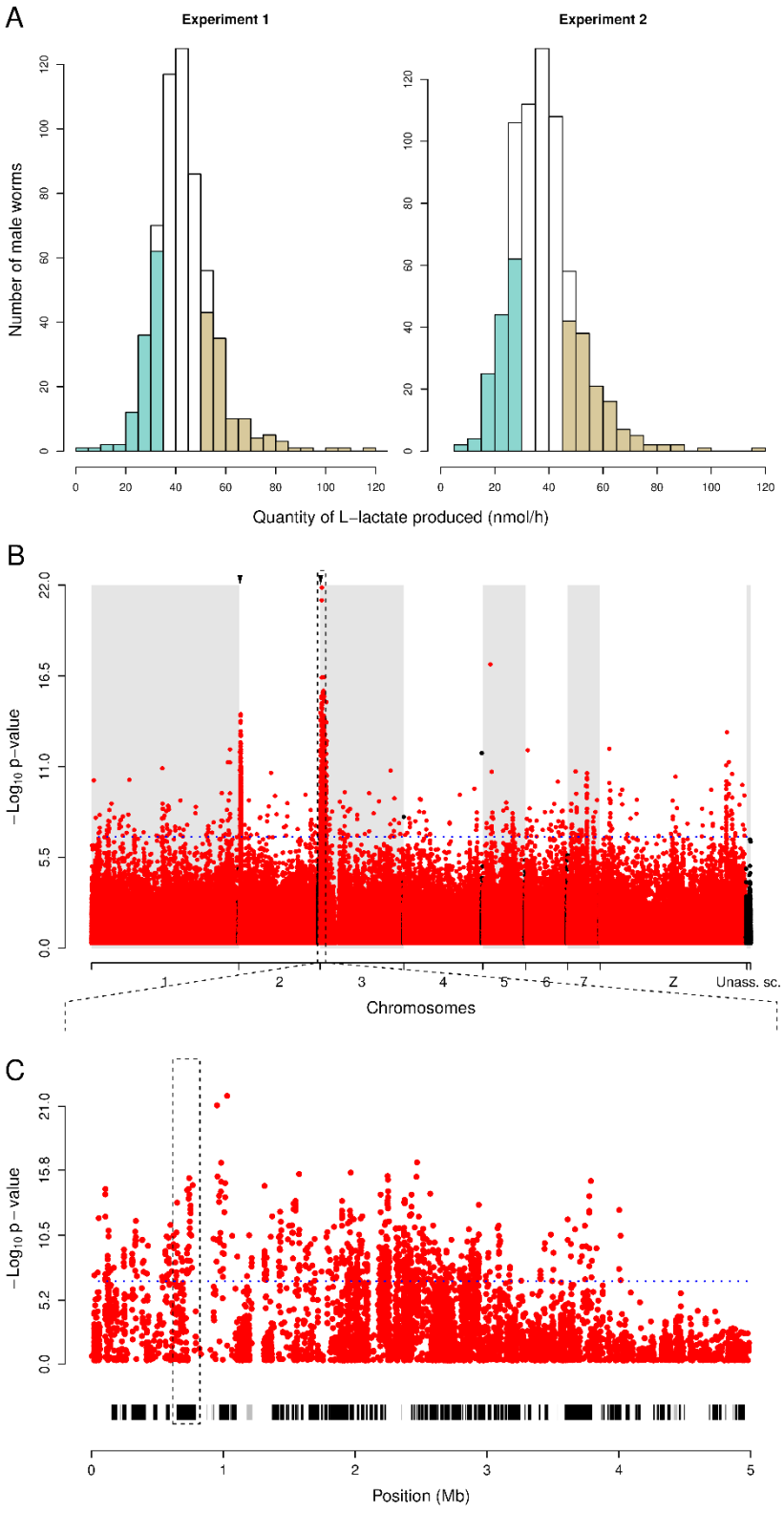

876

877

878 **Fig. 3**

879

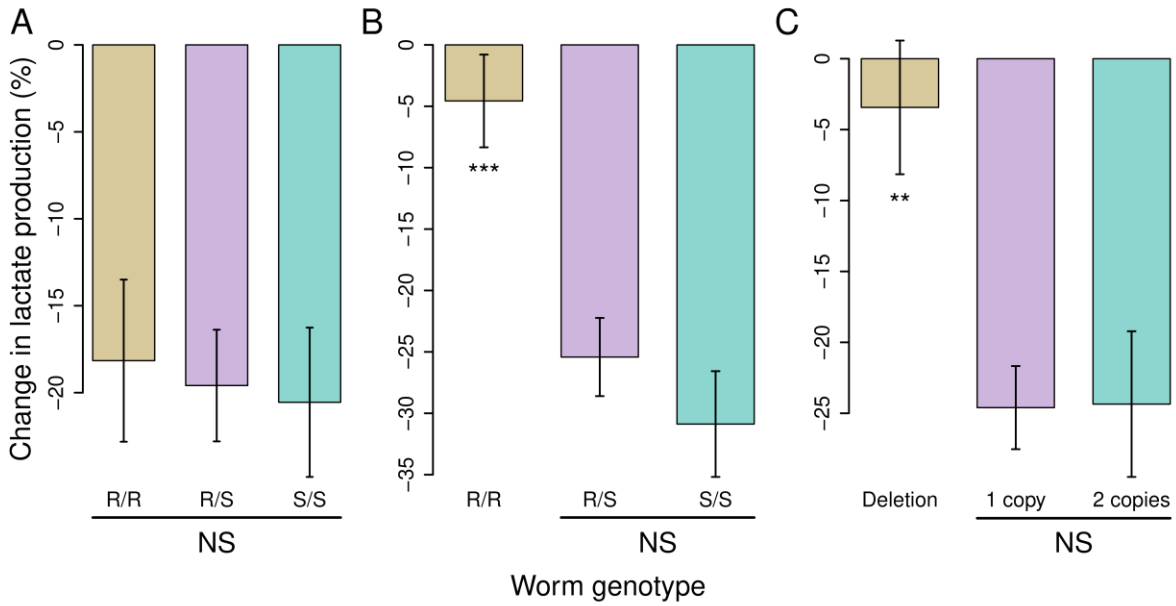

880

881

882 **Fig. 4**

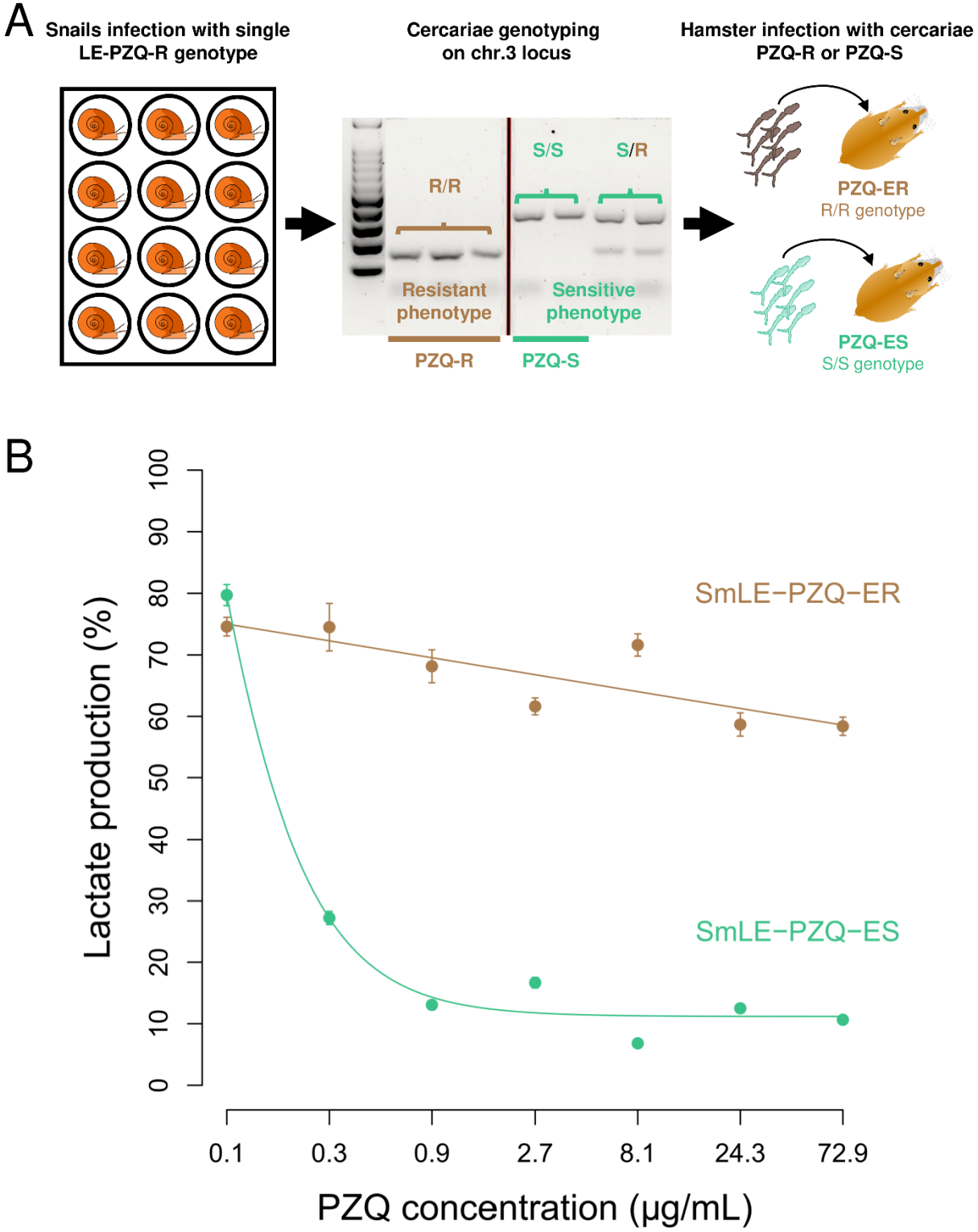

883

884

885 **Fig. 5**

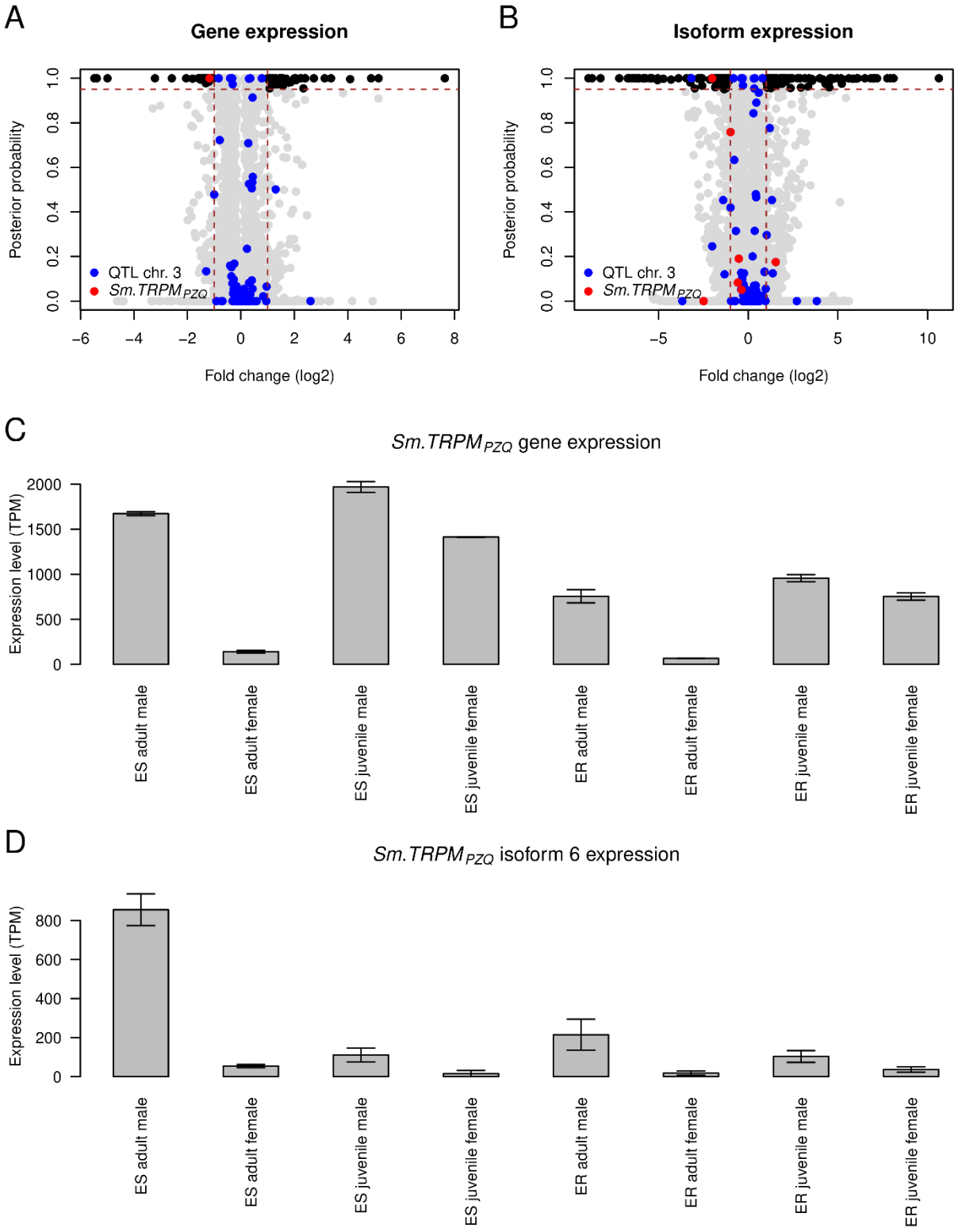

886

887

888 **Fig. 6**

889

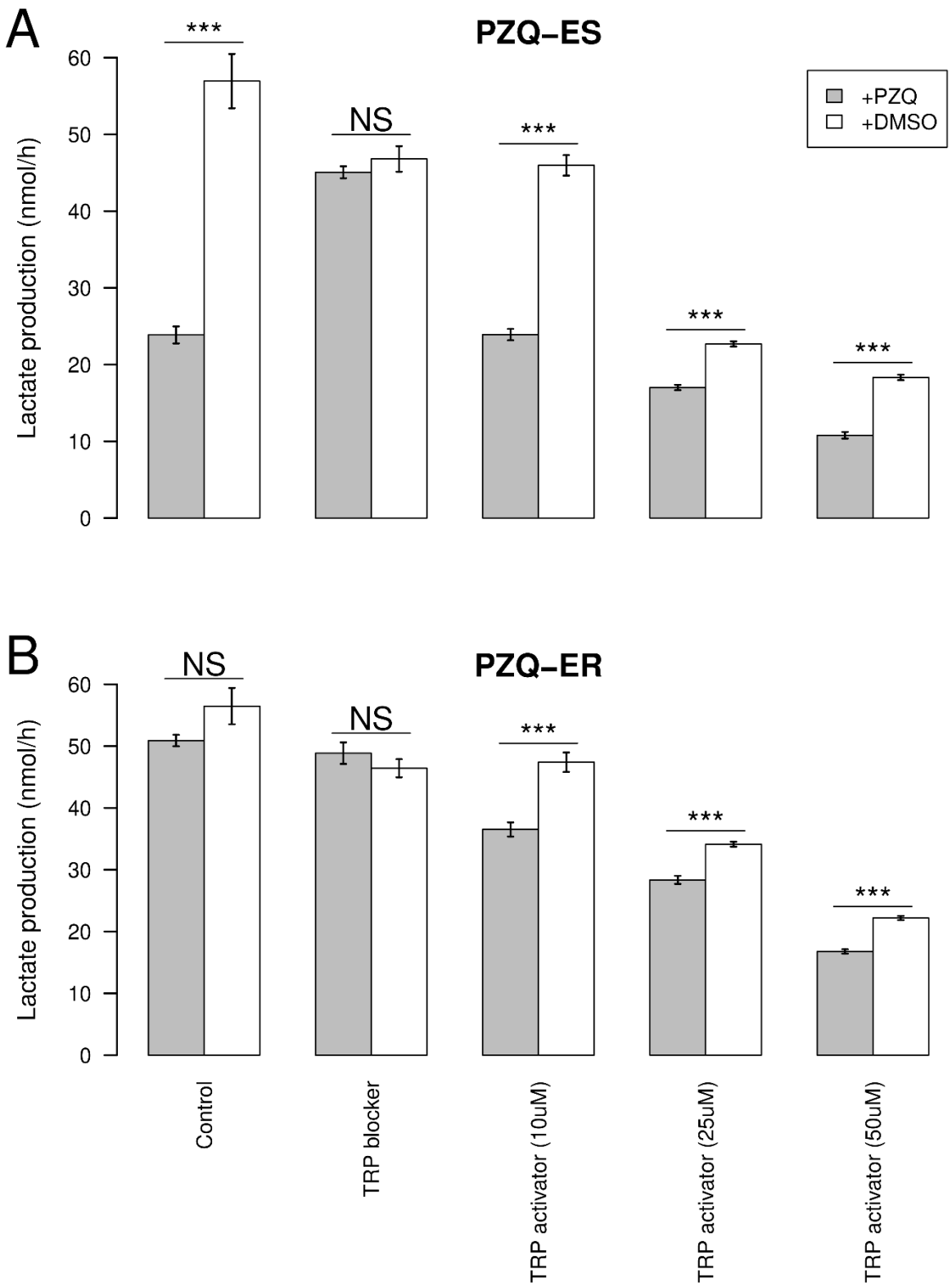

890

File S1.

EXPANDED MATERIALS AND METHODS

Study design

This study was designed to determine the genetic basis of PZQ-R, and was stimulated by the initial observation that a laboratory *S. mansoni* population generated through selection with PZQ contained both PZQ-S and PZQ-R individuals. The project had 6 stages:(i) QTL location. We conducted a genome-wide association study (GWAS). This involved measuring the PZQ-response of individual worms, pooling those showing high levels of resistance and low levels of resistance, sequencing the pools to high read depth, and then identifying the genome regions showing significant differences in allele frequencies between high and low resistance parasites. (ii) Fine mapping of candidate genes. We identified potential candidate genes in these QTL regions, through examination of gene annotations, and exclusion of genes that are not expressed in adults. We also determined whether the loci determining PZQ-R are inherited in a recessive, dominant or co-dominant manner (iii) Marker assisted purification of PZQ-S and PZQ-R parasites. To separate PZQ-R and PZQ-S parasites into "pure" populations, we genotyped larval parasites for genetic markers in the QTL regions and infected rodents with genotypes associated with PZQ-R or PZQ-S. To verify that this approach worked, we then measured the IC_{50} for each of the purified populations. (iv) Characterization of purified SmLE-PZQ-ER and SmLE-PZQ-ES populations. Separation of SmLE-PZQ-ES and SmLE-PZQ-ER parasite populations allowed us to characterize these in more detail. Specifically, we measured expression in juvenile and adult worms of both sexes in both SmLE-PZQ-ES and SmLE-PZQ-ER parasites. We also quantified parasite fitness traits. (v) Functional analysis. We used RNAi and chemical manipulation approaches to modulate activity of candidate genes and determine the impact of PZQ-resistance. We also used transient expression of candidate genes in cultured mammalian cells, to determine the impact of particular SNPs on response to PZQ-exposure. (vi) Survey of PZQ-resistance variants in field collected parasites. Having determined the gene underlying PZQ-R in

laboratory parasites, we examined sequence variation in this gene in a field collection of *S. mansoni* parasites collected to examine the frequency of sequence variants predicted to result in PZQ-resistance.

Ethics statement

This study was performed in accordance with the Guide for the Care and Use of Laboratory Animals of the National Institutes of Health. The protocol was approved by the Institutional Animal Care and Use Committee of Texas Biomedical Research Institute (permit number: 1419-MA and 1420-MU). Details of ethical permission for collection of samples from humans are described in Chevalier et al. *(52)*.

Biomphalaria glabrata *snails and* Schistosoma mansoni *parasites*

Uninfected inbred albino *Biomphalaria glabrata* snails (line Bg121 derived from 13-16-R1 line *(63)*) were reared in 10-gallon aquaria containing aerated freshwater at 26-28 °C on a 12L-12D photocycle and fed *ad libitum* on green leaf lettuce. All snails used in this study had a shell diameter between 8 and 10 mm. We used inbred snails to minimize the impact of snail host genetic background on the parasite life history traits *(66)*.

The SmLE schistosome (*Schistosoma mansoni*) population was originally obtained from an infected patient in Belo Horizonte (Minas Gerais, Brazil) in 1965 and has since been maintained in laboratory *(64)*, using *B. glabrata* NMRI, inbred Bg36 and Bg121 population as intermediate snail host and Syrian golden hamsters (*Mesocricetus auratus*) as definitive hosts. The SmLE-PZQ-R schistosome population was generated in Brazil by applying a single round of PZQ selection pressure on SmLE parasites at both snail and rodent stages *(26)*. The SmLE-PZQ-R population has been maintained in our laboratory using *B. glabrata* NMRI, Bg36 and Bg121 snail population and hamsters as the definitive host since 2014.

Drug resistance tests

Dose-response curves to PZQ in SmLE and SmLE-PZQ-R populations

941 Drug sensitivity to Praziquantel (PZQ) was initially measured using a modified protocol *(65)* in SmLE
942 and SmLE-PZQ-R parasite populations. Ten adult males, recovered by perfusion from infected hamsters
943 (t+ 45 days post-infection) *(69)* from SmLE or SmLE-PZQ-R population were placed into each well of a
944 24-well microplate containing 1 mL of High glucose DMEM supplemented with 15% heat-inactivated
945 fetal bovine serum, 100 U/mL penicillin and 100µg/mL streptomycin (DMEM complete media). We
946 performed control and experimental groups in triplicate (*N*=240 worms/parasite populations). We
947 exposed adult worms to PZQ (0.1 µg/mL, 0.3 µg/mL, 0.9 µg/mL, 2.7 µg/mL, 8.1 µg/mL, 24.3 µg/mL and
948 72.9 µg/mL) for 24h. Worms were then washed three times in drug-free medium and incubated (37°C,
949 5% CO_2) for 2 days. Control groups were exposed only to the drug diluent dimethyl sulfoxide (DMSO).
950 The parasites were observed daily under a stereomicroscope for the 5 days of the experiment and the
951 number of dead worms visually scored. Worms were defined as "dead" if they showed no movements and
952 became opaque. We scored PZQ-resistance as a binary trait: parasites that recovered were classed as
953 resistant, while parasites that failed to recover were classed as sensitive.
954
955 *Metabolic assessment of worm viability using L-lactate assay*
956 We adapted a method for metabolic assessment of worm viability using L-lactate assay *(44)*. Briefly,
957 adult male SmLE-PZQ-R worms recovered from infected hamsters were placed individually in 96-well
958 plates containing 100 µm mesh filter insert (Millipore) in 250 µL DMEM complete media, and allowed to
959 adapt for 24 h. We added PZQ (24.3 µg/mL in DMEM complete media) for the PZQ treated group, while
960 controls were treated with the same volume of drug diluent DMSO. We also added a heat-killed worm
961 control group: adult male worms were placed into a microfuge tube containing distilled water and heated
962 in a dry bath (80°C, 15 min), and then plated in 96-well plate with 100 µm mesh insert. Drug resistance
963 test was conducted as described above (see *Dose-response curves to PZQ in SmLE and SmLE-PZQ-R*
964 *populations*). At 48h post-treatment, the supernatant (125 µL) was collected from each well and
965 immediately stored at -80 °C until processing.

We measured L-lactate levels in the supernatants of *in vitro* treated adult male worms with a colorimetric L-lactate assay kit (Sigma) using 96-well, optical clear-bottom plates (Corning) following the manufacturer's specifications, with minor modifications. Briefly, 5 µL of supernatant were diluted into 20 µL of ddH_2O to fit within the linear range of the assay. We then combine 24 µL of the assay buffer to 1 µL of diluted supernatant (1/5 dilution) in each test well and added 25 µL of the lactate reaction mix (24 µL of the assay buffer, 0.5 µL of enzyme mix and 0.5 µL of lactate assay probe - V_{total}= 50 µL/well). We also made a L-lactate standard curve to allow accurate L-lactate quantification in worm supernatants. After 45 min of incubation in the dark at room temperature, the plate was read by a spectrophotometer (Molecular Devices) at 570 nm. Lactate quantities in worm supernatant were assessed following the manufacturer's instruction, taking in account our dilution factor. All measurement series included a DMEM complete media control to determine the background lactate level, which was then subtracted from the L-lactate quantity of the respective measurements.

Genome wide association analysis and QTL mapping

Schistosome infections

Eggs were collected from livers of hamster infected with SmLE-PZQ-R and hatched under light for 30 min in freshwater to obtain miracidia *(66)*. We then exposed one thousand Bg121 snails to five miracidia/snail. After 30 days, snails were individually exposed to light in 24-well plates to shed cercariae. Eight hamsters were exposed to 840 cercariae (4 cercariae/snail) from a batch of 210 shedding snails. We euthanized hamsters after 45 days to collect adult worms.

Phenotypic selection

Adult SmLE-PZQ-R worms were collected, separated by sex and males were plated individually in 96-well plates (60 worms per plate) containing 100uM mesh filter insert (Millipore) in 250 µL of DMEM complete media and treated with a dose of 24.3 µg/mL PZQ as describe above (i.e. *Metabolic assessment of worms viability using L-lactate assay*). A group of 12 worms were treated with the same volume of

992 drug diluent DMSO. This GWAS experiment was done twice independently. A total of 590 and 691 adult
993 male worms were collected, cultured *in vitro* and exposed to PZQ for the two experiments respectively.
994 Worm media supernatants (125 µL) were collected in 96-well PCR plates after 24h in culture (to
995 assess the viability of the worms before PZQ treatment – adult male worms should release ≥ 40 nmol/h of
996 L-lactate in supernatant) and 48h post-treatment (to assess their viability after PZQ treatment). Plates
997 containing supernatant were immediately stored at -80 °C until processing. Lactate levels in supernatants
998 were quantified as described above (see *Metabolic assessment of worm viability using L-lactate assay*).
999 We phenotype the worms and categorize them into two groups: i) Recovered worms (i.e. releasing ≥ 40
1000 nmol/h of L-lactate in supernatant) and ii) Susceptible worms (i.e. releasing less 40 nmol/h of L-lactate in
1001 supernatant). Among these two groups, we took the 20% of the treated worms releasing in their media the
1002 highest amount of L-lactate (average L-lactate production ± SD: Experiment 1 = 61.44 nmol/h ± 13.16 /
1003 Experiment 2 = 56.38 nmol/h ± 10.82) and the 20% of the treated worms releasing the lowest amount of
1004 L-lactate (average L-lactate production ± SD: Experiment 1 = 28.61 nmol/h ± 5.32 / Experiment 2 =
1005 23.04 nmol/h ± 4.14), 48h post PZQ treatment respectively.
1006
1007 *DNA extraction and library preparation*
1008 We sequenced whole genomes of the two pools of recovered (i.e. resistant to PZQ, Experiment 1: 116
1009 worms / Experiment 2: 137 worms) and susceptible worms (Experiment 1: 116 worms / Experiment 2:
1010 137 worms). We then estimated allele frequencies in each pool to identify genome regions showing high
1011 differentiation.
1012 a. ***gDNA extraction:*** We extracted gDNA from pools of worms using the Blood and Tissue kit
1013 (Qiagen). We homogenized worms in DNA extraction kit lysis buffer using sterile micro pestles.,
1014 incubated homogenates (56 °C, 2 hour) and recovered gDNA in 200 µL of elution buffer. We
1015 quantified the worm gDNA recovered using the Qubit dsDNA HS Assay Kit (Invitrogen).
1016 *b.* ***Whole genome library preparation and sequencing:*** We prepared whole genome libraries from
1017 pools of worm gDNA in triplicate using the KAPA HyperPlus kit (KAPA Biosystems) according

to the manufacturer's protocol. For each library, we sheared 100 ng of gDNA by adaptive focused acoustics (Duty factor: 10%; Peak Incident Power: 175; Cycles per Burst: 200; Duration: 180 seconds) in AFA tubes (Covaris S220 with SonoLab software version 7 (Covaris, Inc., USA)) to recover fragmented DNA (150-200 bp). Library indexing was done using KAPA Dual Adapters at 15 µM for 1h. We used 6 PCR cycles for post-ligation library amplification. We performed size selection on the indexed-amplified libraries using KAPA Pure bead (0.7x first upper size cut; 0.9x second lower size cut). We quantified libraries by qPCR using KAPA library quantification kit (KAPA Biosystems) and their respective fragment size distribution was assessed by TapeStation (Agilent). We sequenced the libraries on a HiSeq X sequencer (Illumina) using 150 bp pair-end reads. Raw sequence data are available at the NCBI Sequence Read Archive (PRJNA699326).

Bioinformatic analysis

Jupyter notebook and scripts used for processing the sequencing data and identifying the QTL are available on Zenodo (DOI: 10.5281/zenodo.5297220).

a. ***Sequence analysis and variant calling:*** We aligned the sequencing data against the *S. mansoni* reference genome (schistosoma_mansoni.PRJEA36577.WBPS14) using BWA (v0.7.17) and SAMtools (v1.10). We used GATK (v4.1.8.1) to mark PCR duplicates and recalibrate base scores. We used the HaplotypeCaller module of GATK to call variants (SNP/indel) and the GenotypeGVCFs module to perform a joint genotyping on each chromosome or unassembled scaffolds. We merged VCF files using the MergeVcfs module. All these steps were automatized using Snakemake (v5.14.0).

b. ***QTL identification:*** We expect the genome region underlying resistance to be enriched in variants from high L-lactate producing worms. To evaluate statistical evidence for such enrichment, we examined the difference in allele frequencies between low and high L-lactate parasites across the genome by calculating a *Z*-score at each bi-allelic site. To minimize bias, we weighed *Z*-scores by including the number of worms in each treatment and the difference in the total read depth across

the triplicated libraries of each treatment at the given variant. We calculated Z-scores for each biological replicate as follows:

$$Z = \frac{p_1 - p_2}{\sqrt{p_0(1-p_0)\left(\frac{1}{x.n_1} + \frac{1}{x.n_2} + \frac{1}{d_1} + \frac{1}{d_2}\right)}}$$

where $p1$ and $p2$ are the estimated allele frequencies in the low and high L-lactate parasites pools, respectively; $p0$ is the allele frequency under the null hypothesis H0: $p1 = p2$ estimated from the average of $p1$ and $p2$; $n1$ and $n2$ are the number of worms in the low and high L-lactate parasites pools, respectively, factor x for each n reflecting the ploidy state (x=2); and $d1$ and $d2$ are the sequencing depths for the low and high L-lactate parasite pools, respectively.

We combined Z-scores generated from each biological replicate as follows:

$$Z_c = \frac{Z_1 + Z_2}{\sqrt{2}}$$

where Z_1 and Z_2 were Z-scores from replicate 1 and 2, respectively. The p-values were obtained by comparing the negative absolute value of Z-scores to the standard normal distribution. To determine the significant threshold, Bonferroni correction was calculated with $\alpha = 0.05$. These analyses are available in the Jupyter notebook and associated scripts (DOI: 10.5281/zenodo.5297220).

Relationship between worm genotype at chr. 2 and 3 and PZQ-R phenotype

To validate the impact of worm genotypes on its PZQ resistance phenotypes and determine whether PZQ-R shows recessive, dominant or codominant inheritance, we determined the PZQ-R phenotype of individual worms, which were then genotyped for markers at the peak of the QTLs located.

Measuring PZQ-R in individual worms

We collected 120 SmLE-PZQ-R adult male worms, plated them individually in 96-well plates containing a mesh filter insert, cultured them *in vitro*, treated them with PZQ (24.3 µg/mL) and collected media supernatants before (after 24h in culture) and 48h post-treatment, and used L-lactate assays to determine PZQ-R status (see *Phenotypic selection*). We extracted gDNA from each worm individually. Briefly, we transferred worms into 96-well PCR plates, added 100 µL of 6% Chelex® solution containing 1% Proteinase K (20 mg/mL), incubated for 2h at 56 °C and 8 min at 100 °C, and transferred the supernatant containing worm gDNA into fresh labeled 96-well plates.

PCR-RFLP conditions for chr.2 and chr.3 loci

We used PCR-RFLP to genotype single worms at loci marking QTL peaks on chr. 2 (C>A, chr SMV7_2: 1072148) and chr. 3 (T>C, chr SMV7_3: 741987). Primers were designed using PerlPrimer v1.21.1 (Table S4). We digested PCR amplicons for chr. 2 with BslI (NEB) and chr. 3 with Mse1 (NEB), and visualized digested PCR amplicons by 2% agarose gel electrophoresis.

Quantitative PCR validation of copy number variation (CNV) in single worms

We genotyped each individual worm for a deletion identified on chr. 3 at position 1220683- 1220861 bp using a custom quantitative PCR assay. This was done to examine the association between deletion of this genomic region and PZQ resistant genotype. We quantified the copy number in this region relative to a single copy gene from *S. mansoni* (α-tubulin 2) *(66)*. The CNV genotype for each parasite corresponds to the ratio of the CNV copy number and the α-tubulin 2 gene copy number: 0=complete deletion, 0.5=one copy, 1=two copies. Methods and primers are described in Table S4. We then compared individual worm phenotypes for each of the three CNV genotypes (0, 1 or 2 copies) to determine the association between CNV and PZQ response.

Marker assisted selection of resistant and susceptible parasite populations

Selection of SmLE-PZQ-ER and SmLE-PZQ-ES populations

We separated the polymorphic SmLE-PZQ-R schistosome population based on chr. 3 QTL genotype using the PCR-RFLP as described. We exposed 960 inbred *B. glabrata* Bg121 snails to one miracidium SmLE-PZQ-R *(66)*. At four weeks post-exposure, we identified infected snail (*N*=272), and collected cercariae from individual snails. We extracted cercarial DNA using 6%Chelex *(66)*), and genotyped each parasite for chr. 3 locus using our PCR-RFLP (Homozygous R/R: n=89 – 36%; Homozygous S/S: n=39 – 16%; Heterozygous R/S: n=117 – 49%) and determine their gender by PCR *(67)*. We selected 32 R/R parasites (homozygous for the *Sm.TRPM*$_{PZQ}$ resistant-associated allele) and 32 S/S genotypes (i.e. homozygous for the *Sm.TRPM*$_{PZQ}$ sensitive-associated allele). For both R/R and S/S we used 13 males and 19 females. We exposed 5 hamsters to 800 cercariae of 32 R/R genotypes parasites and 5 hamsters to 800 cercariae 32 S/S genotyped parasites. This single generation marker assisted selection procedure generates two subpopulations: SmLE-PZQ-ER is expected to be enriched in parasites with R/R genotype and to show strong PZQ-R, while SmLE-PZQ-ES is enriched for S/S genotypes and is expected to be highly sensitive to PZQ).

PZQ IC$_{50}$ *with SmLE-PZQ-ER and SmLE-PZQ-ES*

Forty-five days after exposure to cercariae, we euthanized and perfused hamsters to recover adult schistosome worms from each subpopulation (SmLE-PZQ-ER and SmLE-PZQ-ES). We separated worms by sex and we set adult males in 96-well plates containing 100 µm mesh filter insert (Millipore) and cultured in 250 µL DMEM complete media as described.

We determined PZQ dose-response for both SmLE-PZQ-ER and SmLE-PZQ-ES population. We exposed individual worms (*N*=60/population/treatment) to PZQ (0.1 µg/mL, 0.3 µg/mL, 0.9 µg/mL, 2.7 µg/mL, 8.1 µg/mL, 24.3 µg/mL and 72.9 µg/mL) or drug diluent (DMSO control). Worm media supernatants (125 µL) were collected in 96-well PCR plates before treatment (after 24h in culture) and 48h post-treatment. We quantified L-lactate levels in supernatants described and we assess variation in L-lactate production for each individual worm.

gDNA extraction and library preparation

SmLE-PZQ-ER and SmLE-PZQ-ES parasite populations were maintained in our laboratory. We recovered the F1 worms from each populations and extract gDNA from pools of adult males (100 worms/population) and females (25 worms/population) separately as described above. Post extraction cleaning using Genomic DNA Clean & Concentrator (Zymo) have been performed on female qDNA pools to remove hemoglobin contaminants. We prepared whole genome libraries from these pools in triplicate using the KAPA HyperPlus kit (KAPA Biosystems) as described (see *Whole genome library preparation and sequencing*). We sequenced the libraries on a HiSeq X sequencer (Illumina) using 150 bp paired-end reads. Sequence data are available at the NCBI Sequence Read Archive (accession numbers PRJNA701978).

Bioinformatic analysis

The analysis was identical to the GWAS and QTL mapping analysis. This can be replicated with the Jupyter notebook and associated scripts (DOI: 10.5281/zenodo.5297220).

Fitness of SmLE-PZQ-ER and SmLE-PZQ-ES parasite populations

The SmLE-PZQ-ER and SmLE-PZQ-ES populations of parasites has been maintained in our laboratory using B. glabrata Bg36 and Bg121 snail population and hamster definitive hosts for 12 generations. For each cycle and population, we exposed between 96 to 144 snails with 5-7 miracidia and two hamsters with 700 cercariae. Each generation, we measured snail survival (snails alive/the number of snails exposed) and snail infectivity (snail producing cercariae/number of snails tested for shedding) 4 weeks after miracidial exposure *(66)*. We measured to hamsters for each population of parasites (worms recovered/number of cercariae used to infect each hamster).

Transcriptomic analysis of resistant and susceptible schistosome worms to PZQ at juvenile (28 days) and adult (45 days) stages

Sample collection

Juvenile and adult *S. mansoni* SmLE-PZQ-ER and SmLE-PZQ-ES worms were recovered by perfusion from hamsters at 28 days (juveniles) or 45 days (adults) post-infection. Worms from each population were placed in DMEM complete media, separated by sex, and aliquoted in sterile RNAse free microtubes which were immediately snap-frozen in liquid nitrogen and stored at -80 °C until RNA extractions. For each subpopulation, (SmLE-PZQ-ER or SmLE-PZQ-ES), we collected 3 biological replicates of 30 males and 3 replicates of 30 females for the 28d juvenile worms and 3 biological replicates of 30 males and 3 replicates of 60 females for the 45d adult worms.

RNA extraction and RNA-seq library preparation

a. RNA extraction

We extracted total RNA from all the *S. mansoni* adult and juvenile worms collected using the RNeasy Mini kit (Qiagen). Samples were randomized prior to RNA extraction to minimize batch effects. We homogenized worms in 600 µL RNA lysis buffer (RTL buffer, Qiagen) using sterile micro pestles, followed by passing the worm lysate 10 times through a sterile needle (23 gauge). We recovered total RNA in 25 µL elution buffer. We quantified the RNA recovered using the Qubit RNA Assay Kit (Invitrogen) and assessed the RNA integrity by TapeStation (Agilent - RNA integrity numbers of ~8.5–10 for all the samples).

b. RNA-seq library preparation

We prepared RNA-seq libraries using the KAPA Stranded mRNA-seq kit (KAPA Biosystems) using 500ng RNA diluted in 50uL Tris-HCl (pH 8.0) for each library. We fragmented mRNA (6 min 94°C), indexed libraries using 3'-dTMP adapters (7 µM, 1 hour at 20°C), and used 6 PCR cycles for post-ligation library amplification. We quantified indexed libraries by qPCR (KAPA library quantification kit (KAPA Biosystems)) and assessed their fragment size distribution by TapeStation (Agilent). We sequenced the libraries on a HiSeq 4000 sequencer (Illumina) using 150 bp pair-end reads, pooling 12 RNA-seq

libraries/lane. Raw sequence data are available at the NCBI Sequence Read Archive under accession numbers PRJNA704646.

c. Bioinformatic analysis.

To identify differentially expressed genes between the different groups, we aligned the sequencing data against the *S. mansoni* reference genome (schistosoma_mansoni.PRJEA36577.WBPS14) using STAR (v2.7.3a). We quantified gene and isoform abundances by computing transcripts per million values using RSEM (v1.3.3). We compared these abundances between groups (ES/ER, males/females, juveniles/adults) using the R package EBSeq (v1.24.0). Jupyter notebooks and associated scripts are available on Zenodo (DOI: 10.5281/zenodo.5297218).

Manipulation of Sm.TRPM$_{PZQ}$ channel expression or function:

RNA interference

We used RNA interference to knock down the expression of Smp_246790 gene in order to functionally validate the implication of *Sm.TRPM$_{PZQ}$* on schistosome PZQ resistance. SmLE-PZQ-R adult male worms were freshly recovered from infected hamsters and placed in 24-well plates for in vitro culture (10 adult male worms/well).

a. siRNA treatment on* S. mansoni *adult male worms

Small inhibitory RNAs (siRNAs) targeting specific schistosome genes were designed using the on-line IDT RNAi Design Tool (https://www.idtdna.com/Scitools/Applications/RNAi/RNAi.aspx) (Table S2) and synthesized commercially by Integrated DNA Technologies (IDT, Coralville, IA). To deliver the siRNAs, we electroporated schistosome parasites (10 adults/group – each group done in triplicate) in 100 µL RPMI medium containing 2.5 µg siRNA or the equivalent volume of ddH_2O (no siRNA control), in a 4 mm cuvette by applying a square wave with a single 20 ms impulse, at 125 V and at room temperature (Gene Pulser Xcell Total System (BioRad)) *(70)*. Parasites were then transferred to 1 mL of complete DMEM media in 24-well plates. After overnight culture, medium was replaced with fresh DMEM

complete media. We measured gene expression by quantitative real-time PCR (RT-qPCR) 2 days after siRNA treatment.

b. dsRNA treatment on* S. mansoni *adult male worms

We synthetized double-stranded RNA according to Wang et al. *(71)* (Table S2). For dsRNA treatment, 10 adult male worms/group (each group done in triplicate) were cultured in 1 mL DMEM complete media and treated with 90 ug dsRNA at day 0, day 1 and day 2. Media was changed every 24h and fresh dsRNA was added. On day 3, we harvested worms and measured gene expression by quantitative real-time PCR (RT-qPCR).

c. RNA extraction and gene expression analysis by RT-qPCR

We extracted total RNA from parasites (*N*=10 worms/sample) using the RNeasy Mini kit (Qiagen) (see *RNA extraction*). Complementary DNA (cDNA) was generated from extracted RNA (500 ng - 1 µg) using SuperScript-III and Oligo-dT primers (ThermoFisher). Relative quantification of genes of interest was performed in duplicate by qPCR analysis using QuantStudio 5 System (Applied Biosystems) and SYBR Green master mix (ThermoFisher), compared with a serially diluted standard of PCR products (generated from cDNA) for each of the gene tested *(66)*. Standard curves allow evaluating the efficiency of each pairs of primers, for both housekeeping and target genes using QuantStudio Design and Analysis Software. Expression was normalized to SmGAPDH housekeeping gene (Table S2) using the efficiency $E^{\Delta\Delta Ct}$ method *(72)*.

<u>*Specific Sm.TRPM$_{PZQ}$ chemical inhibitor and activator*</u>

We used specific chemical inhibitor and activators (Chulkov *et al.*, in prep) to manipulate the function of Sm.TRPM$_{PZQ}$ to examine the impact on PZQ-response. We placed individual SmLE-PZQ-ER and SmLE-PZQ-ES adult male worms in 96-well plates with 100 µm mesh filter insert containing DMEM complete media and cultured described above (see *Metabolic assessment of worm viability using L-lactate assay*). After 24h in culture, 20 worms from each population were treated either with a cocktail combining PZQ (1 µg/mL) and i) 50 µM of Sm.TRPM$_{PZQ}$ blocker (ANT1 MB2) or ii) 10 µM, 25 µM or 50 µM of

Sm.TRPM$_{PZQ}$ activator (AG1 MV1) respectively or iii) drug diluent (DMSO). We also set up control plates to evaluate the impact of Sm.TRPM$_{PZQ}$ blocker or activator alone. In that case, 20 worms from each population were treated with a cocktail combining drug diluent DMSO and Sm.TRPM$_{PZQ}$ blocker (MB2) or activator (MV1) at the same concentrations mentioned above. Worms were exposed to these drug cocktails for 24h, washed 3 times with drug-free medium, and incubated (37°C, 5% CO_2) for 2 days.

We collected Worm media supernatants (125 µL) in 96-well PCR plates before treatment (after 24h in culture) and 48h post-treatment and L-lactate levels in supernatants were quantified as described above (see *Metabolic assessment of worm viability using L-lactate assay*). We used these results to determine the impact of blockers or activators on variation in L-lactate production.

In vivo parasite survival after PZQ treatment

We used 24 female Balb/C mice (purchased from Envigo at 6 weeks-old and housed in our facility for one week before use) split into two groups. Each group were exposed by tail immersion to to cercariae from SmLE-PZQ-ER (80 cercariae/mouse from 40 infected snails) or SmLE-PZQ-ES (80 cercariae/mouse from 40 infected snails) population. Each mouse was identified by a unique tattoo ID and an ear punch for assessing treatment status (PZQ or drug diluent control). Immediately after infection, we stained the content of each infection vial with 10 µL 0.4% Trypan blue and counted all the cercarial tails/heads or complete cercariae to determine the cercarial penetration rate for each mouse. We kept infected mice in 4 cages (2 cages/parasite populations and 6 animals per cage) at 21-22° C and 39%–50% humidity and monitored them daily.

Forty days post-infection, we weighed mice and treated them by oral gavage with either 120 mg/kg of PZQ (diluted in 1% DMSO + vegetable oil – Total volume given/mouse: 150 µL) or the same volume of drug diluent only (control group). To minimize batch effects, 3 mice were treated with PZQ and 3 with the drug diluent per cage for each parasite group (SmLE-PZQ-ER or SmLE-PZQ-ES). Mice were monitored daily until euthanasia and perfusion *(69)*, at day 50 post-infection. We recorded the weight of each mouse before euthanasia. After euthanasia and perfusion, we also weighted the liver and

spleen of each individual. We carefully recovered worms from the portal vein, liver and intestine mesenteric venules of each mouse. Worms were separated by sex and counted.

***Sm.TRPM$_{PZQ}$* variants in *S. mansoni* field samples**

Variants identification in exome-sequenced data from natural S. mansoni *parasites*

We utilized exome sequence data from *S. mansoni* from Africa, South America and the middle East to investigate variation in *Sm.TRPM$_{PZQ}$*. African miracidia were from the Schistosomiasis collection at the Natural History Museum (SCAN) *(68)*, Brazilian miracidia and Omani cercariae and adult worms were collected previously. We have previously described methods and generation of exome sequence from *S. mansoni* samples *(51, 52)*. Data were analyzed the same way as described in Chevalier et al. *(52)*. Code is available in Jupyter notebook and scripts (DOI: 10.5281/zenodo.5297222).

Sanger re-sequencing to confirm the presence of the Sm.TRPM$_{PZQ}$ *field variants*

To confirm the presence of the variants in *Sm.TRPM$_{PZQ}$* gene from our exome-sequenced natural *S. mansoni* parasites (when read depth was <10 reads), we performed Sanger re-sequencing of eight *Sm.TRPM$_{PZQ}$* exons (i.e. exon 3, 4, 23, 25, 27, 29 and 34) where either nonsense mutations (leading to truncated protein) or non-synonymous mutation located close to the PZQ binding site *(21)* were identified. Primers and conditions are listed in Table S4.

Sanger sequencing analysis

We scored variants using PolyPhred software (v6.18) (Nickerson et al., 1997) which relies on Phred (v0.020425.c), Phrap (v0.990319), and Consed (v29.0) software, analyzing each exon independently. We identified single nucleotide polymorphisms using a minimum phred quality score (-q) of 25, a minimum genotype score (-score) of 70, and a reference sequence of the *Sm.TRPM$_{PZQ}$* gene from the chromosome 3 of *S. mansoni* reference genome (schistosoma_mansoni.PRJEA36577.WBPS14). Variant sites were labeled as non-reference alleles if they differed from the reference sequence. We identified

insertion/deletion (indel) polymorphisms using a minimum phred quality score (-q) of 25, a minimum genotype score (-iscore) of 70. Polymorphisms were visually validated using Consed. Sanger traces are available on Zenodo (DOI: 10.5281/zenodo.5204523). These analyses are available in the Jupyter notebook and associated scripts (DOI: 10.5281/zenodo.5297222).

Functional analysis

We determined whether proteins produced by variant *Sm.TRPM*$_{PZQ}$ alleles were activated by PZQ following Park et al. *(21)* methods. In brief, we transiently expressed *Sm.TRPM*$_{PZQ}$ in HEK293 hamster cells, exposed transfected cells to PZQ, and measured Ca^{2+} influx to determine activation

Statistical analysis

All statistical analyzes and graphs were performed using R software (v3.5.1). We used the drc package from R to analyze all our dose-response datasets using a four-parameter log-logistic function to fit curves. We used the Readqpcr and Normqpcr packages to analyze all our RT-qPCR datasets, using the *efficiency*$^{\Delta\Delta Ct}$ method. When data were not normally distributed (Shapiro test, $p < 0.05$), we compared results with non-parametric tests: Chi-square test, Kruskal-Wallis test followed by pairwise Wilcoxon-Mann-Whitney post-hoc test or a simple pairwise comparison Wilcoxon-Mann-Whitney test. When data followed a normal distribution, we used one–way ANOVA or a pairwise comparison Welsh *t*-test. The confidence interval of significance was set to 95% and *p*-values less than 0.05 were considered significant.

1293 **SUPPLEMENTARY FIGURES**

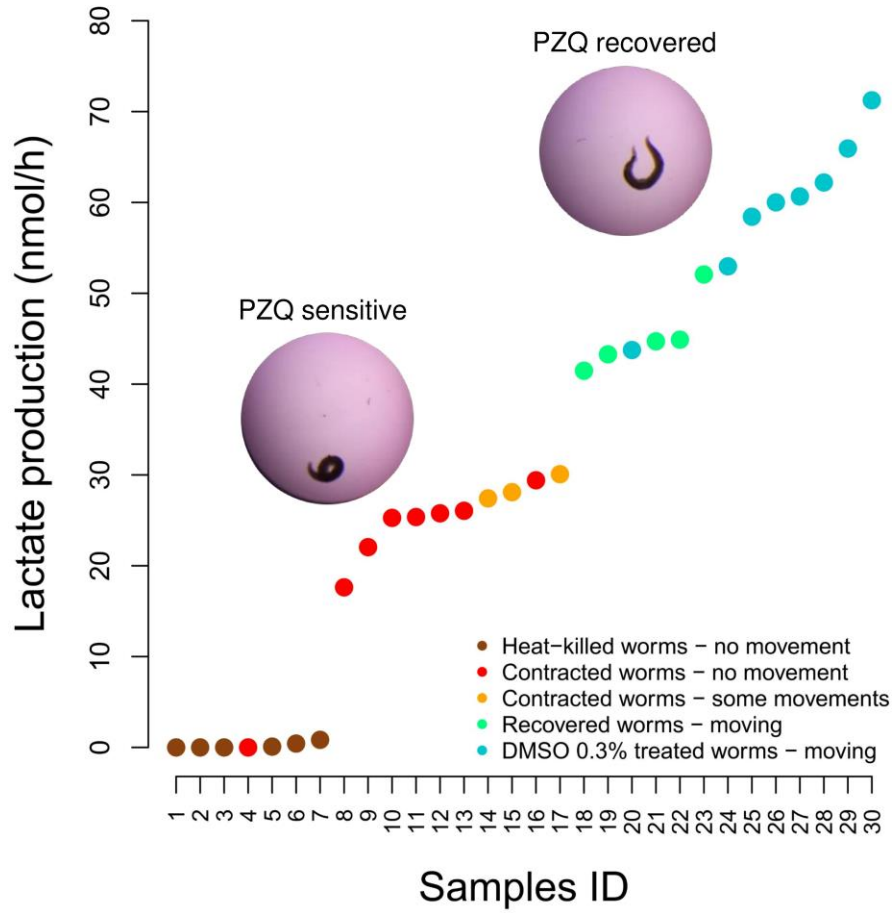

Fig. S1. Development of a L-lactate assay for assaying worm recovery. Validation of the L-lactate assay for single male worms and correlation with their microscopic appearance and ability to regain movement after PZQ treatment (24.3 µg/mL). PZQ-S worms (contracted), that remain contracted after PZQ treatment produce significantly less amount of L-lactate released in the media compared to PZQ-R (recovered and motile) worms (Wilcoxon test, p = 0.0015; *N* = 30 worms).

1294

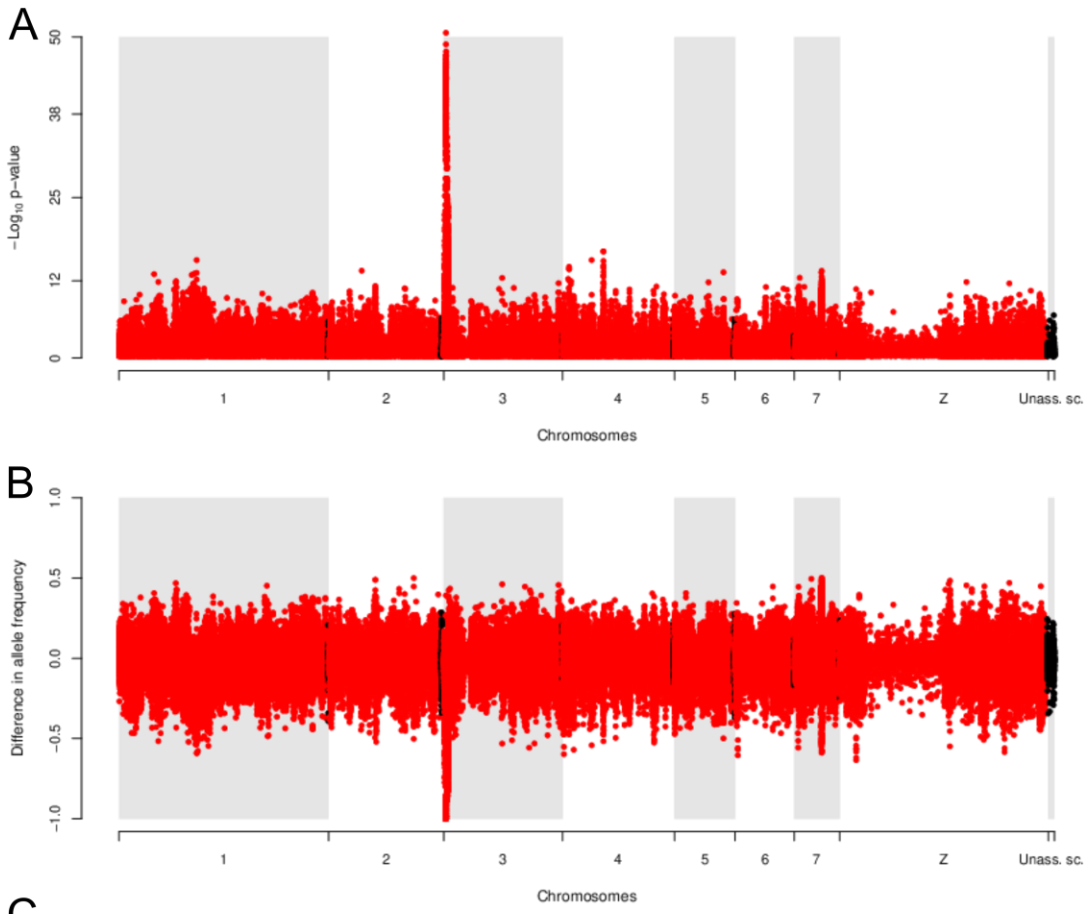

C

Genomic position (bp)	Gene position (bp)	Protein mutation	Allele frequency in PZQ-ER males	Allele frequency in PZQ-ES males	Effect on channel activation
646749	g.597G>GATA	p.N31ins	0.6	0.06	None
724853	g.78701A>ACCG	p.P759ins	0.80	0	Not tested
724861	g.78709C>T	p.P757L	0.76	0	None
724870	g.78718C>CACT	p.L761ins	0.77	0	None
724884	g.78732A>C	p.T765P	0.70	0	Not tested
724887	g.78735T>A	p.S766T	0.79	0	Not tested
741903	g.95751T>A	p.F992L	1	0	None
779144	g.13299G>A	p.R1843Q	1	1	Not tested
779355	g.133203A>AC	p.Q1915PfsX2	0.99	0	Not tested
779359	g.133207C>CA	p.G1916RfsX1	0.01	1	Not tested

Fig. S2. Validation of marker-assisted selection of SmLE-PZQ-ER and ES using Next Generation Sequencing (NGS). SmLE-PZQ-ER and ES differed only at the locus linked to PZQ resistance **(A)** Alternatively fixed allele were fixed for alternative alleles at the *Sm.TRPM*$_{PZQ}$-741987C SNP genotyped (**B**; 1: fixed in ES, -1 fixed in ER), but showed similar allele frequencies across the rest of the genome. Segregating mutations between ER and ES are shown in table **(C)** We determined whether proteins expressing these variations were activated by PZQ following Park *et al*. methods *(21)*.

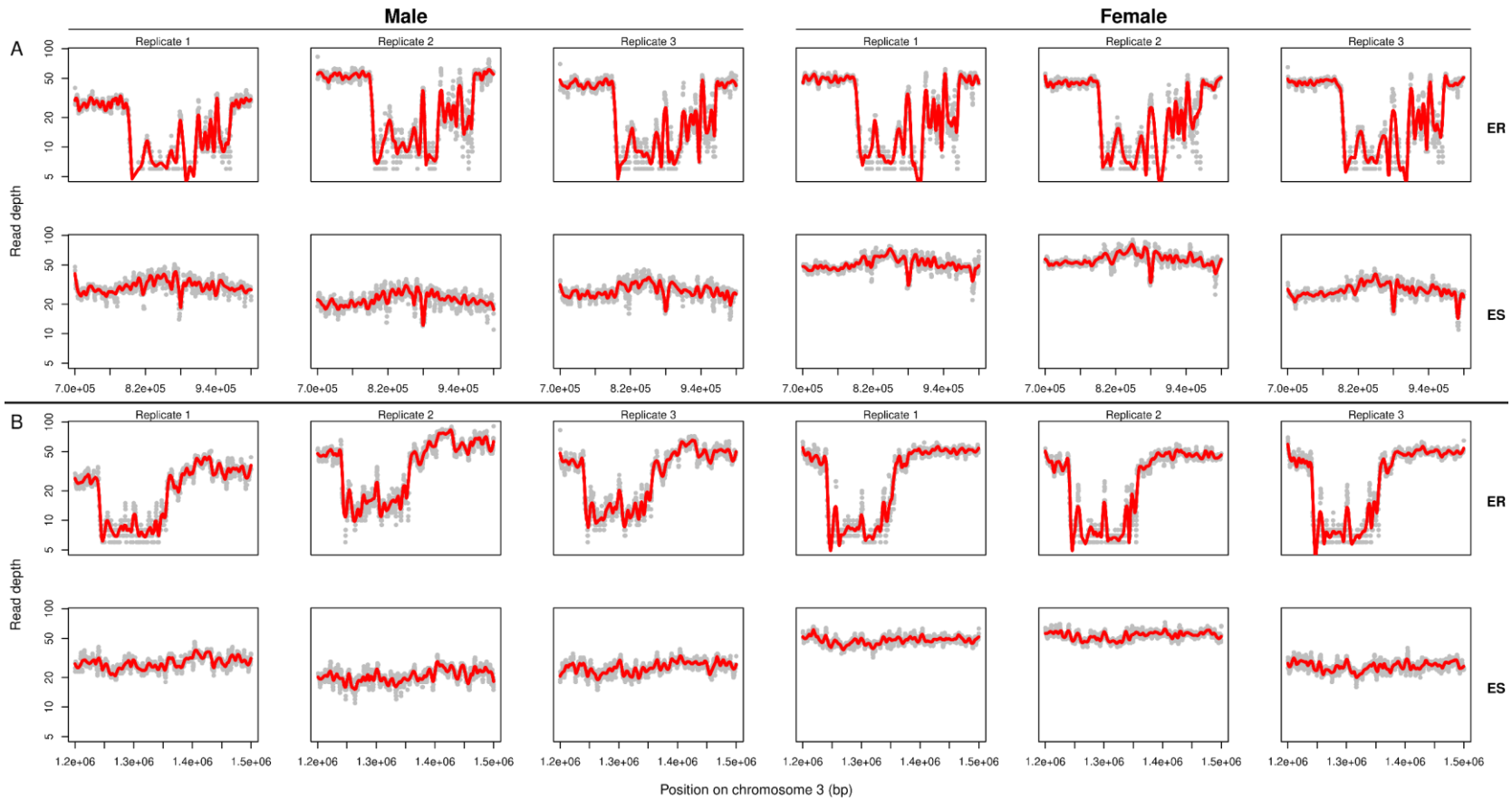

Fig. S3. Large deletions adjacent to *Sm.TRPM*$_{PZQ}$ and SOX13 transcription factor. Sequencing of adult parasites recovered from SmLE-PZQ-ER and SmLE-PZQ-ES populations also revealed that the 100 kb **(A)** and the 150 kb **(B)** deletions were close to fixation in the SmLE-PZQ-ER population. The first row of each panel refers to the ER population, the second to the ES population. The first three columns refer to the female, the last three columns to the males.

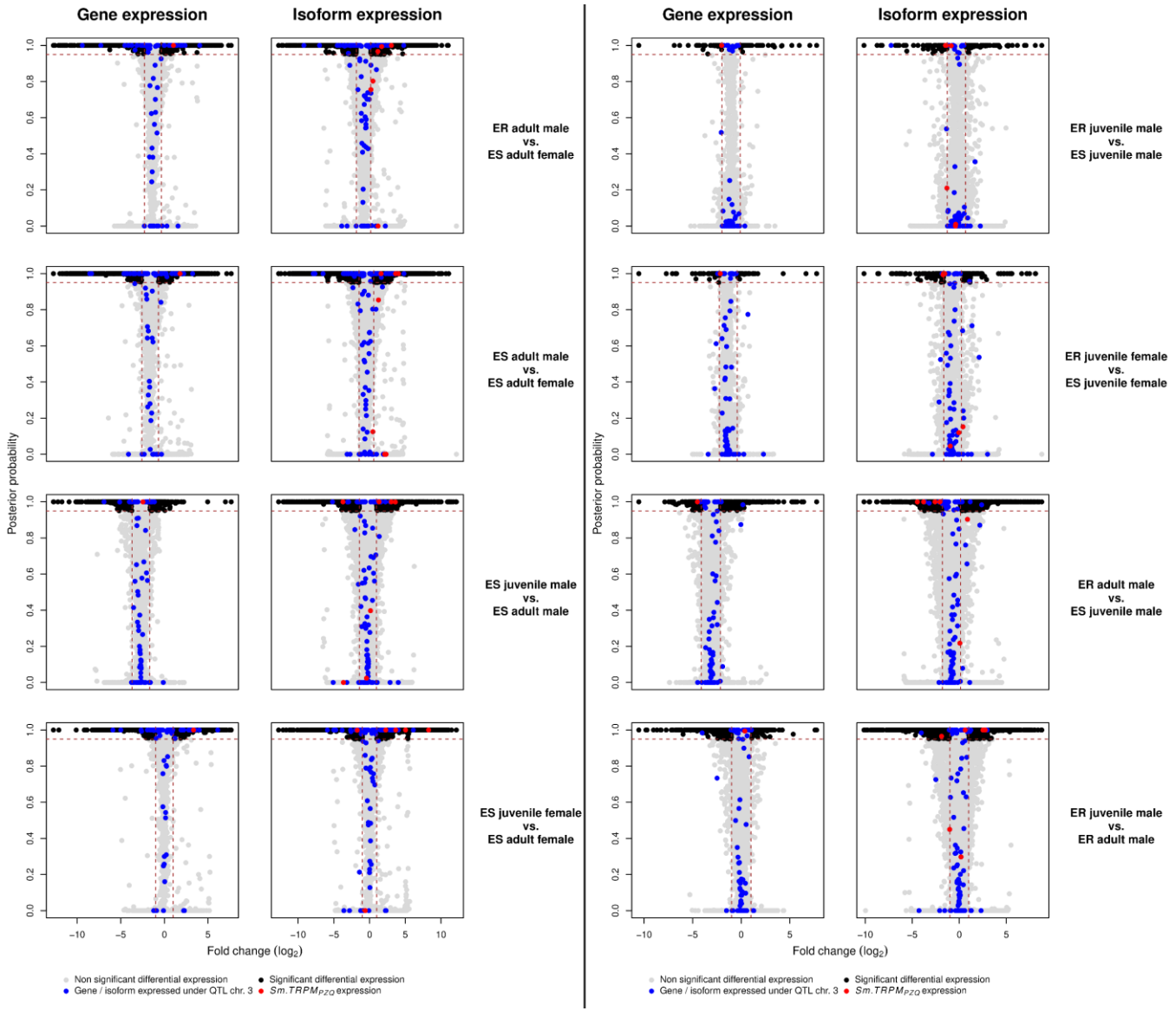

Fig. S4. Detailed genes and isoforms expression in SmLE-PZQ-ER and SmLE-PZQ-ES parasites.
Comparison of genes and isoforms expression between SmLE-PZQ-ER and ES parasites for each sex (i.e. male and female) and each parasite stage (i.e. adult worm and juvenile worm)

1297

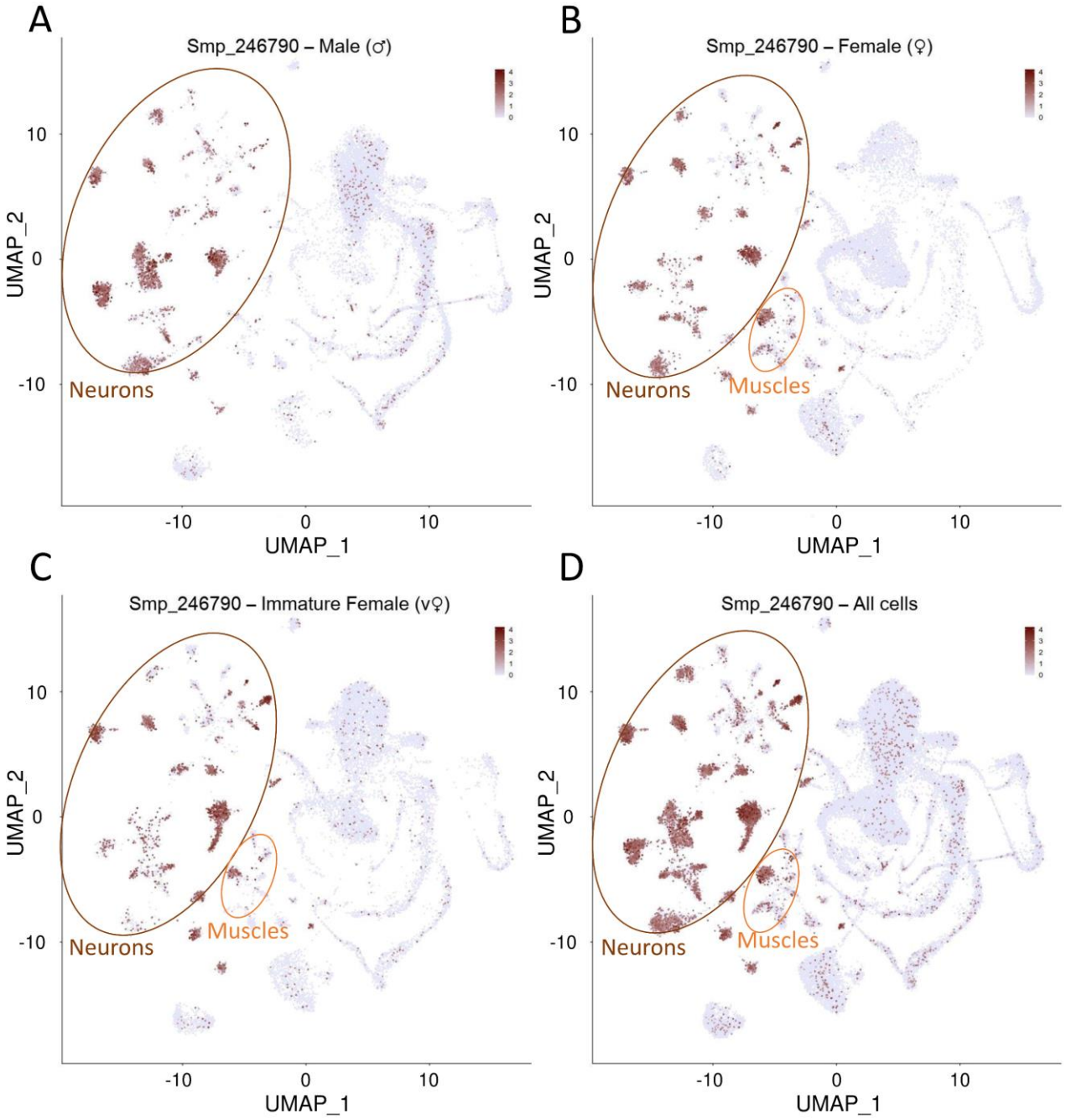

Fig. S5. Cellular localization of *Sm.TRPM$_{PZQ}$* expression in *S. mansoni.* (A) adult male, **(B)** adult female, **(C)** immature female, **(D)** overall sex and stages (SchistoCyte Atlas *(46)*). *Sm.TRPM$_{PZQ}$* gene is essentially expressed in neurons for all sex and stages and is also expressed in muscle cells in females.

1298

1299

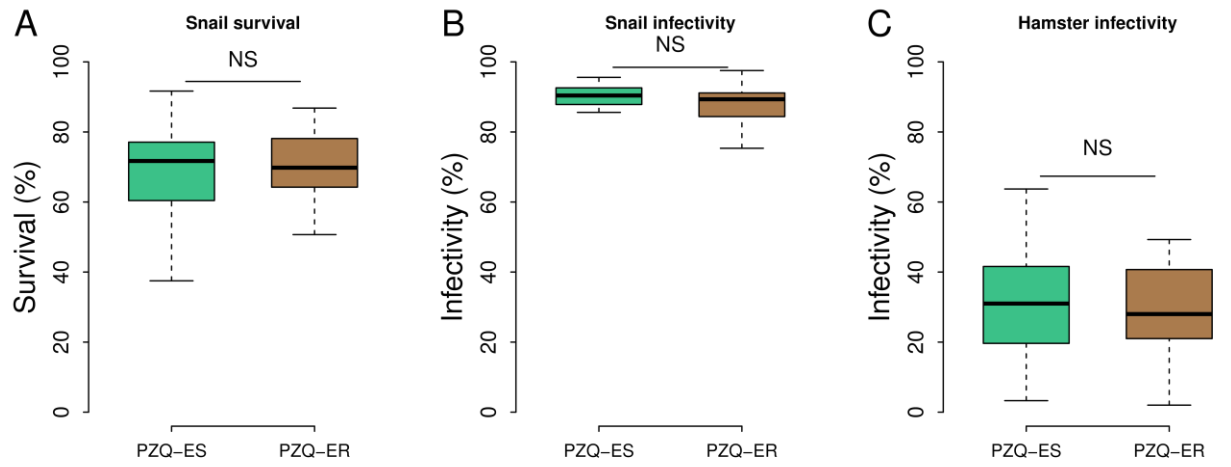

Fig S6. Fitness of SmLE-PZQ-ES and SmLE-PZQ-ER parasites. Comparison of several life history traits: **(A)** Snail survival (Welsh t-test, t = -0.662, p = 0.51), **(B)** infectivity to snails (Wilcoxon test, W = 123, p = 0.45), and **(C)** infectivity to hamsters (Welsh t-test, t = 0.725, p = 0.47) for 12 generations of SmLE-PZQ-ER and SmLE-PZQ-ES parasites. (NS: No significant difference between groups).

1300

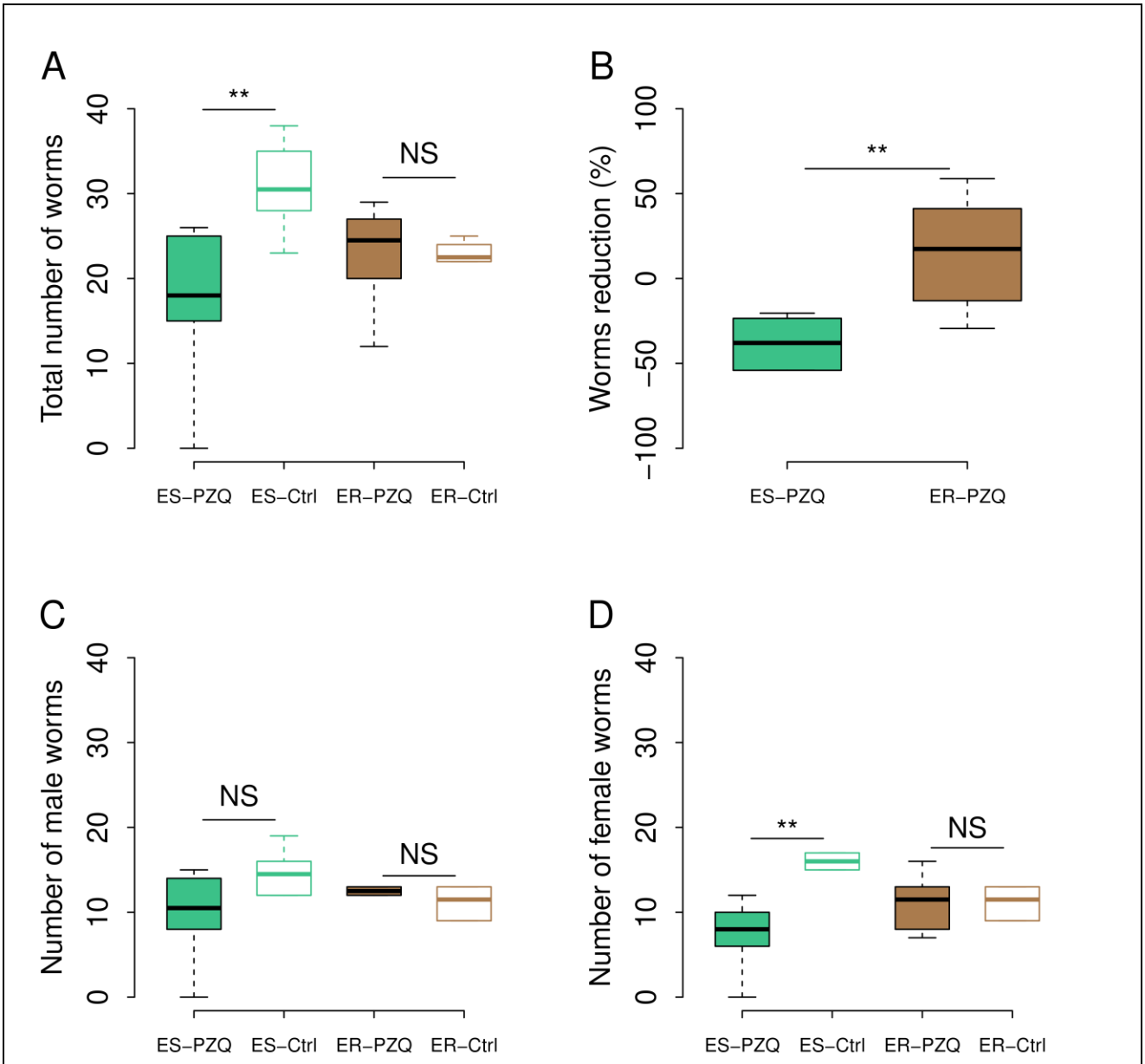

Fig. S7. Impact of *in vivo* PZQ treatment on SmLE-PZQ-ER and SmLE-PZQ-ES parasites. Balb/c mice were infected with either SmLE-PZQ-ER or SmLE-PZQ-ES parasites populations and treated with 120 mg/kg of PZQ or DMSO (control group). **(A)** We observed no significant reduction in worm burden in SmLE-PZQ-ER parasites when comparing PZQ-treated and control (DMSO) treated animals (Wilcoxon test, p = 0.393). In contrast, we recovered significantly lower numbers of worms from PZQ-treated versus untreated mice infected with the SmLE-PZQ-ES parasite population (Wilcoxon test, p = 0.008). **(B)** The percent reduction observed was significantly different between the SmLE-PZQ-ES and SmLE-PZQ-ER parasites (Wilcoxon test, p = 0.0129). **(C)** While Interestingly, we did not reach significance for male worms (Wilcoxon test, p = 0.089), **(D)** we observed a large reduction in numbers of female worms recovered from PZQ-treated SmLE-PZQ-ES parasites relative to untreated animals (Wilcoxon test, p = 0.008) (N = 24 mice – 6 mice/group; NS: No significant difference between groups; *$p < 0.05$; ** $p \leq 0.02$; *** $p \leq 0.002$).

1301

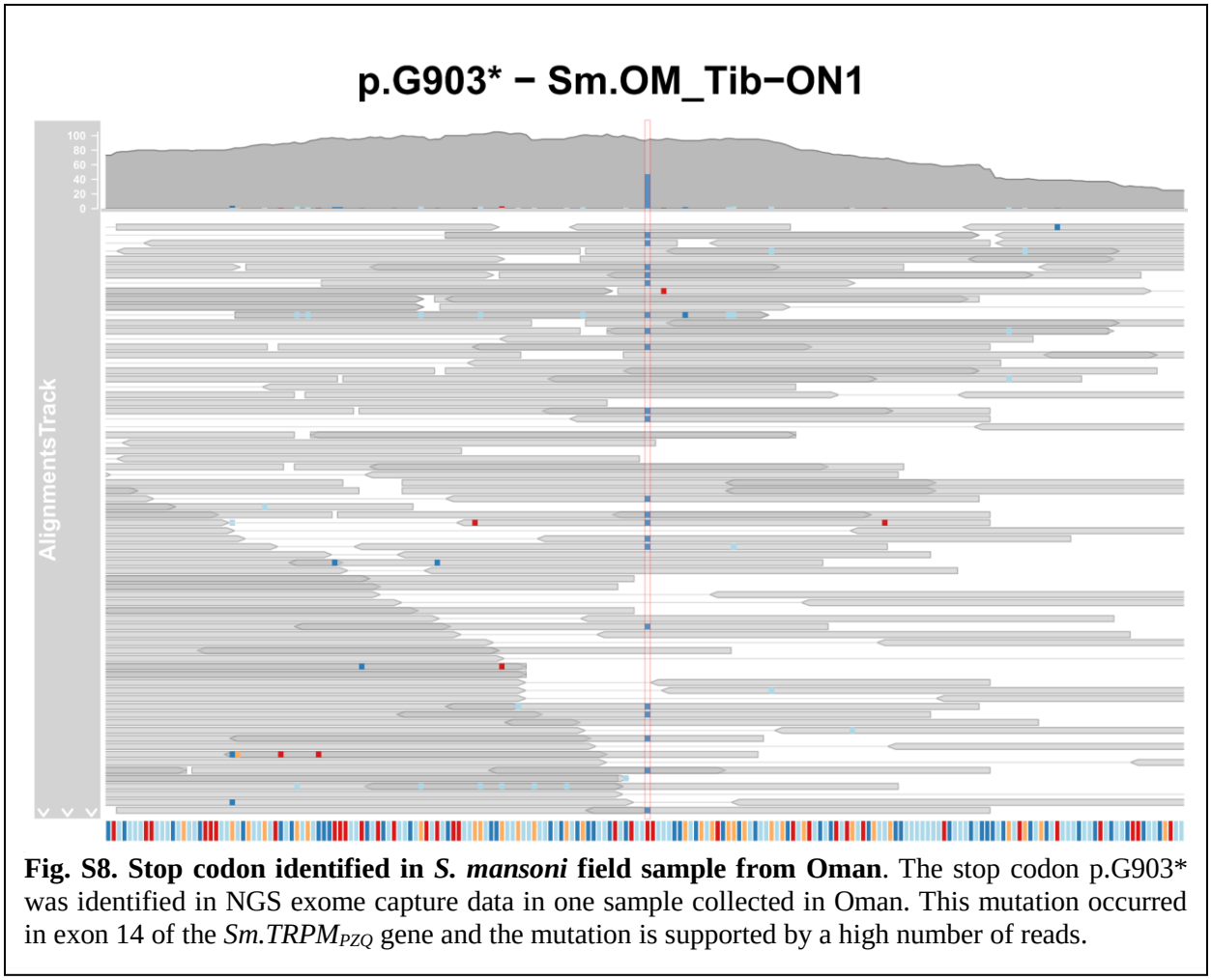

Fig. S8. Stop codon identified in *S. mansoni* field sample from Oman. The stop codon p.G903* was identified in NGS exome capture data in one sample collected in Oman. This mutation occurred in exon 14 of the *Sm.TRPM*$_{PZQ}$ gene and the mutation is supported by a high number of reads.

1302

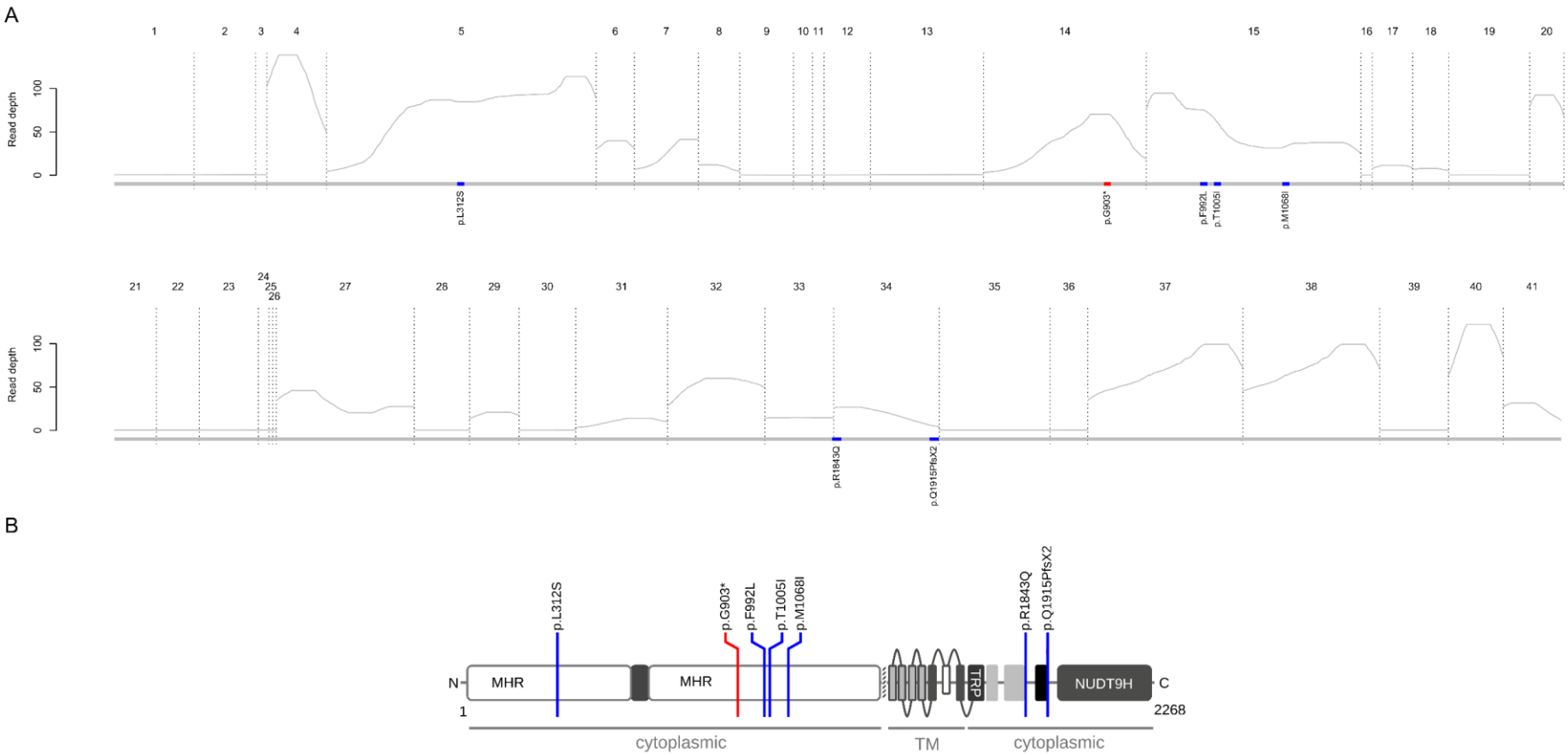

Fig. S9. *Sm.TRPM$_{PZQ}$* gene: average exon read depth and identified mutations in field samples. (A) Exons are numbered and delimited with dotted lines. Blue boxes on the grey line represent positions of the high frequency mutations. Red box represents the position of the low frequency resistant mutation. Mutation position mentioned below the boxes refers to the isoform 5. **(B)** Mutations were reported to the schematic structure of Sm.TRPM$_{PZQ}$ modified from *(20)*. The resistant mutation is located before the transmembrane domain (TM) leading to no a non-functional channel (MHR: TRPM homology region, TRP: TRP domain, NUDT9H: human ADP-ribose (ADPR) pyrophosphatase).

Table S1. Genes in QTL regions on chr 2 and 3.

Separate file

Table S2. Summary table of RNAi for Sm.TRPM$_{PZQ}$. siRNA sequences and primers used to generate dsRNA. Primer sequences used for RT-qPCR to quantify gene expression after RNAi treatment on worms (Chr.: Chromosome; E: Exon). * siRNA negative (scramble siRNA) and positive control (SmAP) have been used from Krautz-Peterson *et al. (70)*.

Location on the genome	Genomic coordinates	Type	Sequence (5'-3' orientation)	Expected size (bp)	Usage
Chr. 3	646335-646359	siRNA SmTRP #1 (isoform 5) E1-E2	AGUACUUUGUUGAAGUCCUUGAATA	-	siRNA
Chr. 3	724927-724951	siRNA SmTRP #2 (isoform 5) E10-E20	CAGCAUUUUUAGAAUGUGAUAAATA	-	siRNA
Chr. 3	767394-767415	siRNA SmTRP #3 (isoform 6) E23-E32	ACCAAGGAGAAUAUGACAUUGAATT	-	siRNA
Chr. 4	33713410-33713434	siRNA SmAP* (positive control)	CCACAAGCAUGUUCUCUUACAUACA	-	siRNA
-	-	Scrambled siRNA* (negative control)	CUUCCUCUCUUUCUCUCCCUUGUGA	-	siRNA
Chr. 3	646449-646472	dsRNA SmTRP #1 (isoform 1-5) – Forward primer	GAAACTGGTACTTTATCCAAGTCC	614	dsRNA generation
Chr. 3	685256-685276	dsRNA SmTRP #1 (isoform 1-5) – Reverse primer	TCAGCTGCTTTCCATAAACCT		dsRNA generation
Chr. 3	700008-700029	dsRNA SmTRP #2 (isoform 6) – Forward primer	TACAAGTCAACAAAGTGGACCT	602	dsRNA generation
Chr. 3	706699-706721	dsRNA SmTRP #2 (isoform 6) – Reverse primer	CTTCAATGATGGATTCAAGCCTG		dsRNA generation
-	-	EGFP Forward primer primer with T7 promoter (negative control)	GGTAATACGACTCACTATAGGGAGGTAAACGGCCACAAGTTCAG	591	Control RNAi (dsRNA)
-	-	EGFP Reverse primer with T7 promoter (negative control)	GGTAATACGACTCACTATAGGGAGGTGCTCAGGTAGTGGTTGTC		Control RNAi (dsRNA)
Chr. 3	756865-756887	SmTRP_qF1– Forward primer	AGTCCTACTTCTGAACAACAAGG	124	RT-qPCR
Chr. 3	757787-757808	SmTRP_qR1– Reverse primer	TATATTCCACGGTTCTAGCCTG		RT-qPCR

Chr. 3	787906-787927	SmTRP_qF2 pyrophosphatase domain (isoform 6) – Forward primer	ATCAGCAGTTTGATTACACGTC	199	RT-qPCR
Chr. 3	791384-791407	SmTRP_qR2 pyrophosphatase domain (isoform 6) – Reverse primer	GAAGTTGAGCTCCTTTACTTTCAG		RT-qPCR
Chr. 4	3371912 4-3371914 7	SmAP_qF1 – Forward primer	TCAACTCAGATAGACTCACAACAG	76	RT-qPCR
Chr. 4	3372031 8-3372033 8	SmAP_qR1 – Reverse primer	TTAAATGGCCCTTTCACACCT		RT-qPCR
Chr. 1	4316475 5-4316477 1	SmGAPDH_qF2 - Forward primer	CATTGATAAAGCTCAGGCTCAT	195	RT-qPCR
Chr. 1	4316453 9-4316456 2	SmGAPDH_qR2 - Reverse primer	AACTTATCATGAATGACCTTAGCC		RT-qPCR

1309

Table S3. Mutations present in *Sm.TRPM*$_{PZQ}$ in natural schistosome populations from 3 African countries (Senegal, Niger, Tanzania), the Middle East (Oman) and South America (Brazil).

Separate file

Table S4. Summary table of all the primer sequences used for i) PCR-RFLP and CNV quantification for single worm genotyping, ii) Sanger sequencing of Sm.TRPM$_{PZQ}$ in field collected *S. mansoni* parasites (Chr. : Chromosome; E: Exon).

Location on the genome	Genomic coordinates	Exon coordinate (Gene exon number)	Type	Sequence (5'-3' orientation)	Expected size (bp)	Usage
Chr. 2	1071798-1071820	-	Chr. 2 PCR-RFLP – Forward primer	GACAAGAACCCATCAAGTAACAT	618	PCR-RFLP genotyping[a]
Chr. 2	1072394-1072415	-	Chr. 2 PCR-RFLP – Reverse primer	GACAAAGCTACCACAACAAACT		PCR-RFLP genotyping[a]
Chr. 3	741747-741766	-	Chr. 3 PCR-RFLP – Forward primer	TCGTAATAAACATGGTCGTC	421	PCR-RFLP genotyping[a]
Chr. 3	742148-742167	-	Chr. 3 PCR-RFLP – Reverse primer	TCGACTACAGAATGATGTAA		PCR-RFLP genotyping[a]
Chr. 3	1220683-1220701	-	Chr. 3 CNV genotyping – Forward primer	GAAACATTCTGGTCCACCC	179	CNV genotyping (qPCR) [b]
Chr. 3	1220840-1220861	-	Chr. 3 CNV genotyping – Reverse primer	TGGCTTCAGTATTGAAAGTTGC		CNV genotyping (qPCR) [b]
Chr. 4	46055234-46055257	-	Chr. 4 α-tubulin 2 – Forward primer	CGACTTAGAACCAAATGTTGTAGA	190	qPCR (CNV relative quantification) [b]
Chr. 4	46055405-46055424	-	Chr. 4 α-tubulin 2 – Reverse primer	GTCCACTACATTGATCCGCT		qPCR (CNV relative quantification) [b]
Chr. 3	693769-693788	693738-693904 (4)	Sm.TRPM$_{PZQ}$ E 3 – Sanger sequencing – Forward primer	AGGAGTAATGAAGCTAACTG	140	Sanger sequencing[c]
Chr. 3	693891-693909	693738-693904 (4)	Sm.TRPM$_{PZQ}$ E 3 – Sanger sequencing – Reverse primer	GTTACCTCATGTAAAGCTG		Sanger sequencing[c]
Chr. 3	699775-699792	699733-700482 (5)	Sm.TRPM$_{PZQ}$ E 4 – Sanger sequencing – Forward primer	GCTGAAGATAGTGAACCA	271	Sanger sequencing[c]
Chr. 3	700027-700046	699733-700482 (5)	Sm.TRPM$_{PZQ}$ E 4 – Sanger sequencing – Reverse primer	TGTGTTGTAGAACTGATAGG		Sanger sequencing[c]
Chr. 3	764334-764354	764295-764594 (27)	Sm.TRPM$_{PZQ}$ E 23 – Sanger sequencing – Forward primer	GATGGATGGAATAAATTAGAT	288	Sanger sequencing[c]
Chr. 3	764603-764622	764295-764594 (27)	Sm.TRPM$_{PZQ}$ E 23 – Sanger sequencing – Reverse primer	CAACATAGAAACAAATCAAA		Sanger sequencing[c]

Chr. 3	771992-772011	772107-772214 (29)	Sm.TRPM$_{PZQ}$ E 25 – Sanger sequencing – Forward primer	ATAATGCTTGATTCCCTTCC	345	Sanger sequencing[c]
Chr. 3	772318-772337	772107-772214 (29)	Sm.TRPM$_{PZQ}$ E 25 – Sanger sequencing – Reverse primer	TAATCCCACATAGATGACAG		Sanger sequencing[c]
Chr. 3	774815-774832	774968-775167 (31)	Sm.TRPM$_{PZQ}$ E 27 – Sanger sequencing – Forward primer (1)	CTCCATCAGGAGAAACAG	418	Sanger sequencing[c]
Chr. 3	775214-775233	774968-775167 (31)	Sm.TRPM$_{PZQ}$ E 27 – Sanger sequencing – Reverse primer (1)	AAGTATCGTGGCTTATTAGG		Sanger sequencing[c]
Chr. 3	774815-774832	774968-775167 (31)	Sm.TRPM$_{PZQ}$ E 27 – Sanger sequencing – Forward primer (2)	CTCCATCAGGAGAAACAG	459	Sanger sequencing[c]
Chr. 3	775255-775274	774968-775167 (31)	Sm.TRPM$_{PZQ}$ E 27 – Sanger sequencing – Reverse primer (2)	GTACACTTAATTCGTACGAC		Sanger sequencing[c]
Chr. 3	778437-778454	778446-778595 (33)	Sm.TRPM$_{PZQ}$ E 29 – Sanger sequencing – Forward primer	ATGACTCAGGGTATTGGA	287	Sanger sequencing[c]
Chr. 3	778706-778724	778446-778595 (33)	Sm.TRPM$_{PZQ}$ E 29 – Sanger sequencing – Reverse primer	GGGTTGATGGATATTTGGG		Sanger sequencing[c]
Chr. 3	787904-787924	787852-788001 (38)	Sm.TRPM$_{PZQ}$ E 34 – Sanger sequencing – Forward primer	TTATCAGCAGTTTGATTACAC	116	Sanger sequencing[c]
Chr. 3	788001-788020	787852-788001 (38)	Sm.TRPM$_{PZQ}$ E 34 – Sanger sequencing – Reverse primer	CATTATGTTCTATCCATACC		Sanger sequencing[c]

[a] PCR condictions for RFLP genotyping: reactions contained 9.325 µL sterile water, 1.5 µL 10x buffer, 1.2 µL dNTP (2.5 mM each), 0.9 µL $MgCl_2$, 0.5µL each primer (10 µM), 0.075 µL *Taq* polymerase (TaKaRa) and 1µL of gDNA template using the following program: 95 °C for 5 minutes, [95 °C for 30s, 55 °C for 30s, and 72 °C for 1min] × 35 cycles, 72 °C for 10 minutes.

[b]qPCR genotpring methods: we conducted qPCR in duplicate for each reaction (samples and standards). Reactions consisted of 5 µL SYBR Green PCR master mix (Applied Biosystems), 3.4 µL sterile water, 0.3 µL of each primer and 1 µL of standard PCR product or sample gDNA. We used the following program: 95 °C for 10 minutes, [95 °C for 15s and 60 °C for 1 minute] × 40 cycles followed by a melting curve step (15s at 95 °C and then rising in 0.075 °C increments/second from 60 °C to 95 °C), to check for the uniqueness of the product amplified. We plotted standard curves using seven 10-fold dilutions of a purified i) α-tubulin 2 PCR product (α-tubulin 2 copies. µL−1: 2.21×10^{2} – 2.21×10^{7}, efficiency= 87.56%) and ii) CNV region PCR product (Sm.CNV region copies. µL−1: 8.40×10^{1} – 8.40×10^{6}, efficiency= 86.17%). PCR products for standard curves were generated as described in LeClech *et al. (66)*. The number of CNV region and α-tubulin 2 copies in each sample was estimated according to the standard curve (QuantStudio Design and Analysis Software). All the primers were designed using PerlPrimer v1.21.1.

[c]PCR conditions for Sanger sequencing: PCRs were performed using the TaKaRa Taq kit (Clontech, USA). For Exon 25 and 27, PCR reactions contained 8.325 µL sterile water, 1.5 µL 10X buffer, 1.2 µL dNTP (2.5 mM each), 0.9 µL $MgCl_2$ (25 mM), 0.5 µL each primer (10 µM), 0.075 µL Taq polymerase (5 U/µL) and 2 µL of DNA template (WGA DNA from *S. mansoni* field collected miracidia from infected patients) (Total reaction volume: 15 µL). For Exon 3, 4, 12, 23, 29 and 34, PCR reactions were done in a total volume of 50 µL (keeping similar volume ratio between the reagents) with 2 µL of DNA template. We used a SimpliAmp Thermal cycler (Applied Biosystems) with the following program: 95 °C for 5 min; 95 °C for 30 s, 53 °C for 45 s, 72 °C for 45 s, for 35 cycles; then 72 °C for 10 min. We verified the presence and size of all PCR products on 2% agarose gels. Ten microliters of PCR products were then cleaned up by adding 4 µL of ExoSAP-IT (Affymetrix USB products) and 2 µL of sterile water and Sanger sequenced in both directions.